Measurements of absolute branching fractions of $D^{0(+)} \to KKK\pi$ decays

M. Ablikim *et al.*[*]
(BESIII Collaboration)

(Received 24 October 2025; accepted 21 August 2026; published 5 November 2026)

Using an e^+e^- sample of 20.3 fb^{-1} collected at a center-of-mass energy $\sqrt{s} = 3.773$ GeV with the BESIII detector, we report measurements of several four-body hadronic decays of D mesons. All studied decay modes are dominated by Cabibbo-favored amplitudes. The absolute branching fractions are determined to be $\mathcal{B}(D^0 \to K^0_S K^0_S K^0_S \pi^0) = (7.8^{+2.3}_{-2.0} \pm 1.5) \times 10^{-5}$, $\mathcal{B}(D^0 \to K^0_S K^+ K^- \pi^0) = (18.4^{+2.6}_{-2.5} \pm 2.4) \times 10^{-5}$, $\mathcal{B}(D^0 \to K^0_S K^0_S K^- \pi^+) = (12.9^{+1.7}_{-1.6} \pm 1.3) \times 10^{-5}$, $\mathcal{B}(D^0 \to K^0_S K^0_S K^+ \pi^-) = (5.7^{+1.2}_{-1.1} \pm 1.0) \times 10^{-5}$, $\mathcal{B}(D^0 \to K^+ K^- K^- \pi^+) = (17.4^{+1.8}_{-1.7} \pm 2.2) \times 10^{-5}$, $\mathcal{B}(D^+ \to K^0_S K^0_S K^0_S \pi^+) = (6.0^{+2.1}_{-1.7} \pm 1.6) \times 10^{-5}$, and $\mathcal{B}(D^+ \to K^0_S K^+ K^- \pi^+) = (13.8^{+2.4}_{-2.2} \pm 2.5) \times 10^{-5}$. Furthermore, significant ϕ signals are found in the decay channels involving a K^+K^- pair, and their fractions are determined as $\mathcal{B}(D^0 \to \phi K^0_S \pi^0)/\mathcal{B}(D^0 \to K^0_S K^+ K^- \pi^0) = (61^{+15}_{-14} \pm 10)\%$, $\mathcal{B}(D^0 \to \phi K^- \pi^+)/\mathcal{B}(D^0 \to K^+ K^- K^- \pi^+) = (71^{+10}_{-10} \pm 13)\%$, and $\mathcal{B}(D^+ \to \phi K^0_S \pi^+)/\mathcal{B}(D^+ \to K^0_S K^+ K^- \pi^+) = (59^{+22}_{-19} \pm 9)\%$. The branching fractions of $D^0 \to K^0_S K^0_S K^0_S \pi^0$, $D^0 \to K^0_S K^+ K^- \pi^0$, and $D^+ \to K^0_S K^0_S K^0_S \pi^+$ are measured for the first time, and those of $D^0 \to K^0_S K^0_S K^- \pi^+$, $D^0 \to K^0_S K^0_S K^+ \pi^-$, $D^0 \to K^+ K^- K^- \pi^+$, $D^0 \to \phi K^- \pi^+$, and $D^+ \to K^0_S K^+ K^- \pi^+$ are measured with improved precision. The first uncertainties are statistical and the second are systematic.

DOI: 10.1103/pwtz-p7vb

I. INTRODUCTION

Hadronic decays of charmed mesons provide a unique laboratory for studying the interplay between weak interactions and nonperturbative strong dynamics in the charm-quark sector [1,2]. Multibody decays, with their rich phase space, are sensitive to final-state interactions, which can significantly influence decay rates [3].

Since the discovery of D mesons in the 1970s, branching fractions of D decays have been investigated extensively and precisely [4]. However, the $D^{0(+)} \to KKK\pi$ decays remain poorly explored. To date, the most precise measurements of these decays come from the FOCUS experiment, which measured the branching fractions of $D^0 \to K^+K^-K^-\pi^+$ [5] and $D^+ \to K^0_S K^+ K^- \pi^+$ [6] as well as the combined branching fraction of $D^0 \to K^0_S K^0_S K^- \pi^+$ and $D^0 \to K^0_S K^0_S K^+ \pi^-$ [7] relative to $D^0 \to K^0_S \pi^+ \pi^-$ with large uncertainty. Other multibody decays, such as $D^0 \to K^0_S K^+ K^- \pi^0$, have not been measured. Experimentally, previous studies of these decays have been challenging due to the low reconstruction efficiencies, high background and limited data samples, since the branching fractions are suppressed by the small available phase space.

In this paper, we report the new measurements of the absolute branching fractions of $D^0 \to K^0_S K^0_S K^0_S \pi^0$, $D^0 \to K^0_S K^+ K^- \pi^0$, $D^0 \to K^0_S K^0_S K^- \pi^+$, $D^0 \to K^0_S K^0_S K^+ \pi^-$, $D^0 \to K^+ K^- K^- \pi^+$, $D^+ \to K^0_S K^0_S K^0_S \pi^+$, and $D^+ \to K^0_S K^+ K^- \pi^+$ by analyzing e^+e^- collision data corresponding to an integrated luminosity of 20.3 fb^{-1} [8], collected at a center-of-mass energy of $\sqrt{s} = 3.773$ GeV with the BESIII detector. In addition, we also measure the branching fractions of the ϕ-dominated modes $D^0 \to \phi K^0_S \pi^0$, $D^0 \to \phi K^- \pi^+$, and $D^+ \to \phi K^0_S \pi^+$. Throughout this paper, charge conjugate processes are always implied.

II. BESIII DETECTOR AND MONTE CARLO SIMULATION

The BESIII detector is a magnetic spectrometer [9] located at the Beijing Electron Positron Collider (BEPCII) [10]. The cylindrical core of the BESIII detector consists of a helium-based multilayer drift chamber (MDC), a plastic scintillator time-of-flight system (TOF), and a CsI (Tl) electromagnetic calorimeter (EMC), which are all enclosed in a superconducting solenoidal magnet providing a 1.0 T magnetic field.

The solenoid is supported by an octagonal flux-return yoke with resistive plate counter muon identification modules interleaved with steel. The charged-particle momentum resolution at 1 GeV/c is 0.5%, and the specific

[*]Full author list given at the end of the article.

Published by the American Physical Society under the terms of the Creative Commons Attribution 4.0 International license. Further distribution of this work must maintain attribution to the author(s) and the published article's title, journal citation, and DOI. Funded by SCOAP[3].

energy loss dE/dx resolution is 6% for electrons from Bhabha scattering. The EMC measures photon energies with a resolution of 2.5% (5%) at 1 GeV in the barrel (end cap) region. The time resolution in the TOF barrel region is 68 ps, while that in the end cap region was 110 ps. The end cap TOF system was upgraded in 2015 using multigap resistive plate chamber technology, providing a time resolution of 60 ps, which benefits 86% of the data used in this analysis [11–13].

Monte Carlo (MC) simulated data samples, produced with a Geant4-based [14] software package including the geometric description of the BESIII detector and the detector response, are used to determine the detection efficiency and estimate the backgrounds. The simulation includes the beam-energy spread and initial-state radiation in the e^+e^- annihilations modeled with the generator KKMC [15].

An inclusive MC sample consists of the production of $D\bar{D}$ pairs, the non-$D\bar{D}$ decays of the $\psi(3770)$, the initial-state radiation production of the J/ψ and $\psi(3686)$ states, and the continuum processes, and is used for background study. The known decay modes including tag modes $D \to K\pi$, $D \to K\pi\pi$, and $D \to K\pi\pi\pi$ are modeled with EvtGen [16,17] using the branching fractions taken from the Particle Data Group (PDG) [4,18–20], and the remaining unknown decays are estimated with LUNDCHARM [21,22].

The signal MC samples for all decays are generated with possible intermediate resonant contributions. The models of tag decays are the same as those implemented in the inclusive MC sample of $\psi(3770)$. For the signal side, each $D^0 \to K^0_S K^0_S K\pi$ decay mode is generated with a phase-space (PHSP) model. For $D \to K^+K^-K\pi$, the signal MC samples are generated as mixtures of $D \to \phi K\pi$, $D \to \phi K^*(892)$, $D \to K^+K^-K^*(892)$, and nonresonant $D \to K^+K^-K\pi$. For $D \to \phi K\pi$, the MC samples are generated as mixtures of $D \to \phi K\pi$ and $D \to \phi K^*(892)$. The mixing ratios for the signal decays $D^0 \to K^+K^-K^-\pi^+$ and $D^0 \to \phi K^-\pi^+$ are taken from the PDG [4], while those for other decays are determined by studying the invariant mass distributions of the K^+K^-, $K^-\pi^+$, $K^\pm\pi^0$, and $K^0_S\pi^\pm$ in data.

In all simulated samples, final-state radiation from charged particles is modeled using PHOTOS package [23].

III. MEASUREMENT METHOD

The $D^0\bar{D}^0$ or D^+D^- pairs are produced without any additional hadron in e^+e^- annihilations at $\sqrt{s} = 3.773$ GeV. This process provides a clean environment to measure the branching fractions of hadronic D decays using the double-tag (DT) method [24]. First, single-tag (ST) candidates are selected by reconstructing a $\bar{D}^0$ or D^- in the following hadronic final states: $\bar{D}^0 \to K^+\pi^-$, $K^+\pi^-\pi^0$, $K^+\pi^+\pi^-\pi^-$, and $D^- \to K^+\pi^-\pi^-$, $K^0_S\pi^-$, $K^+\pi^-\pi^-\pi^0$, $K^0_S\pi^-\pi^0$, $K^0_S\pi^+\pi^-\pi^-$, $K^+K^-\pi^-$. Events in which a signal candidate is selected in the presence of an ST $\bar{D}$ meson are called DT events. The branching fractions of the $D^0 \to K^0_S K^0_S K^0_S\pi^0$, $D^0 \to K^0_S K^+K^-\pi^0$, $D^0 \to K^0_S K^0_S K^-\pi^+$, $D^0 \to K^0_S K^0_S K^+\pi^-$, $D^0 \to K^+K^-K^-\pi^+$, $D^+ \to K^0_S K^0_S K^0_S\pi^+$, and $D^+ \to K^0_S K^+K^-\pi^+$ are determined by

$$\mathcal{B}_{\rm sig} = N_{\rm DT}/(N^{\rm tot}_{\rm ST} \cdot \epsilon_{\rm sig}), \tag{1}$$

where $N^{\rm tot}_{\rm ST} = \sum_i N^i_{\rm ST}$ and $N_{\rm DT}$ are the total ST yield and the signal yield in the data, respectively, and $N^i_{\rm ST}$ is the ST yield of the tag mode i. The efficiency $\epsilon_{\rm sig}$ of detecting the signal D decay, averaged over all tag modes i, is given by

$$\epsilon_{\rm sig} = \sum_i (N^i_{\rm ST} \cdot \epsilon^i_{\rm DT}/\epsilon^i_{\rm ST})/N^{\rm tot}_{\rm ST}, \tag{2}$$

where $\epsilon^i_{\rm ST}$ and $\epsilon^i_{\rm DT}$ are the efficiencies of detecting ST and DT candidates in the tag mode i, respectively. To cancel potential correlated systematic uncertainties, the branching fractions of $D^0 \to \phi K^0_S\pi^0$, $D^0 \to \phi K^-\pi^+$, and $D^+ \to \phi K^0_S\pi^+$ are measured relative to $D^0 \to K^0_S K^+K^-\pi^0$, $D^0 \to K^+K^-K^-\pi^+$, and $D^+ \to K^0_S K^+K^-\pi^+$, respectively, given by

$$\mathcal{B}_{\rm relative} = \frac{\mathcal{B}^{D\to\phi K\pi}_{\rm sig}}{\mathcal{B}^{D\to KKK\pi}_{\rm sig}} = \frac{N^{D\to\phi K\pi}_{\rm DT} \cdot \epsilon^{D\to KKK\pi}_{\rm sig}}{N^{D\to KKK\pi}_{\rm DT} \cdot \epsilon^{D\to\phi K\pi}_{\rm sig}}. \tag{3}$$

Here, $N^{D\to\phi K\pi}_{\rm DT}$ and $N^{D\to KKK\pi}_{\rm DT}$ denote the signal yields of $D \to \phi K\pi$ and $D \to KKK\pi$, respectively, while $\epsilon^{D\to\phi K\pi}$sig and $\epsilon^{D\to KKK\pi}$sig represent their corresponding detection efficiencies.

The measured branching fractions of neutral D decays need to be corrected for quantum correlation (QC) effects which are present in the data but are not implemented in the MC simulation. This correction is necessary because the $D^0\bar{D}^0$ pairs are produced in a coherent quantum state, and the tagged final state $K^+\pi^-$ can originate from either a Cabibbo-favored $\bar{D}^0 \to K^+\pi^-$ decay or a doubly Cabibbo-suppressed $D^0 \to K^+\pi^-$ decay. The interference between these amplitudes, combined with the quantum correlation, alters the observed decay rates [25]. Analogous effects apply to all D^0 tag modes employed in this analysis. Due to limited signal yields in this analysis, the QC effect for D^0 decays is considered as a source of systematic uncertainty.

IV. EVENT SELECTION

The selection criteria for $K^\pm$, $\pi^\pm$, K^0_S, and π^0 are adopted from Ref. [26]. All charged tracks, except those originating from K^0_S decays, are required to have a polar angle θ with respect to the symmetry axis of the MDC within the MDC acceptance, $|\cos\theta| < 0.93$, and a distance of closest approach to the interaction point (IP) within 10 cm along the beam direction and within 1 cm in the plane

perpendicular to the beam direction. Particle identification (PID) for charged pions and kaons is performed by using TOF information and the $\mathrm{d}E/\mathrm{d}x$ measured by the MDC to calculate confidence levels for the pion and kaon hypotheses (CL_π and CL_K). Kaon and pion candidates are identified via $CL_K > CL_\pi$ and $CL_\pi > CL_K$, respectively.

The K_S^0 candidates are formed with two oppositely charged tracks, which are assigned the pion hypothesis without applying PID criteria. Due to the long lifetime of the K_S^0 meson, the distance of closest approach to the IP in the beam direction must be less than 20 cm, and there is no requirement for the distance of closest approach in the plane transverse to the beam direction. The two charged tracks are constrained to originate from a common vertex with a flight distance from the IP at least twice the vertex resolution. To improve the mass resolution, the K_S^0 decay-vertex fit and the secondary vertex fit with respect to the IP must satisfy $\chi^2 < 100$, with the number of degrees of freedom (n.d.f.) equal to 1 for the K_S^0 vertex fit and 2 for the secondary vertex fit. The invariant mass of $\pi^+\pi^-$ is required to be within $(0.487, 0.511)$ GeV/c^2 ($M_{K_S^0}^{\mathrm{nominal}} \pm 3\sigma_{\mathrm{resolution}}$).

The π^0 candidates are formed with photon pairs. The photon candidates are identified using isolated showers in the EMC. The deposited energy of each shower must be more than 25 MeV in the barrel region ($|\cos\theta| < 0.80$) and more than 50 MeV in the end cap region ($0.86 < |\cos\theta| < 0.92$). To exclude showers that originate from charged tracks, the angle subtended by the EMC shower and the position of the closest charged track at the EMC must be greater than 10 degrees as measured from the IP. To suppress electronic noise and showers unrelated to the event, the difference between the EMC time and the event start time is required to be within [0, 700] ns. Photon pairs with an invariant mass in the range of $(0.115, 0.150)$ GeV/c^2 ($M_{\pi^0}^{\mathrm{nominal}} \pm 3\sigma_{\mathrm{resolution}}$), are taken as π^0 candidates. To improve the mass resolution, a kinematic fit constraining the invariant mass of $\gamma\gamma$ to the nominal π^0 mass [4] is applied, and the resulting χ^2 of the fit is required to be less than 50 with n.d.f. $= 1$.

In the selection of $\bar{D}^0 \to K^+\pi^-$ tag candidates, backgrounds from cosmic rays and Bhabha events are rejected with the same requirements as in Ref. [27]. The TOF time difference between the two charged tracks is required to be less than 5 ns. The track pair must not be consistent with being a muon or electron-positron pair. Additionally, there must be at least one EMC shower with a deposited energy of more than 50 MeV, or at least one additional charged track detected in the MDC.

V. YIELDS OF ST $\bar{D}$ MESONS

The tagged $\bar{D}$ mesons are identified using two variables, namely the energy difference

$$\Delta E_{\mathrm{tag}} \equiv E_{\mathrm{tag}} - E_{\mathrm{beam}}, \tag{4}$$

and the beam-constrained mass

$$M_{\mathrm{BC}}^{\mathrm{tag}} \equiv \sqrt{E_{\mathrm{beam}}^2/c^4 - |\vec{p}_{\mathrm{tag}}|^2/c^2}. \tag{5}$$

Here, E_{beam} is the beam energy, and $\vec{p}_{\mathrm{tag}}$ and E_{tag} are the momentum and the energy of the $\bar{D}$ candidate in the rest frame of the e^+e^- system, respectively. For each tag mode, if there are multiple candidates in an event, only the one with the minimum $|\Delta E_{\mathrm{tag}}|$ is kept. The measurements are performed in events containing at least one ST $\bar{D}$ candidate. Although the ST and DT selections both start with an ST candidate and use the same tag-side multiple-candidate selection, the tag-side environment, e.g., the track multiplicity, may differ between ST and DT events. This tag bias therefore does not fully cancel in the ST and DT selection, and is considered as a source of systematic uncertainty.

The tagged $\bar{D}$ candidates must fulfill mode-dependent ΔE_{tag} requirements due to different resolutions, as listed in the second columns of Tables I and II.

To determine the ST yields of $\bar{D}$ mesons for individual tag modes, unbinned maximum-likelihood fits are performed to the $M_{\mathrm{BC}}^{\mathrm{tag}}$ distributions of the ST candidates, following the procedure described in Ref. [26]. In the fits, the $\bar{D}$ signal is modeled by an MC-simulated shape convolved with a Gaussian function with free parameters accounting for the resolution difference between data and MC simulation. The resulting fits on the $M_{\mathrm{BC}}^{\mathrm{tag}}$ distributions for different tag modes are shown in Fig. 1. The extracted

TABLE I. The ΔE_{tag} requirements, ST yields (N_{ST}), ST efficiencies (ϵ_{ST}) and DT efficiencies (ϵ_{DT}) for D^0 decays. The superscripts 1–7 identify the signal decays: $^1D^0 \to K_S^0K_S^0K_S^0\pi^0$, $^2D^0 \to K_S^0K^+K^-\pi^0$, $^3D^0 \to \phi K_S^0\pi^0$, $^4D^0 \to K_S^0K_S^0K^-\pi^+$, $^5D^0 \to K_S^0K_S^0K^+\pi^-$, $^6D^0 \to K^+K^-K^-\pi^+$ and $^7D^0 \to \phi K^-\pi^+$. The uncertainties are statistical only.

Tag mode	ΔE_{tag} (MeV)	N_{ST} ($\times 10^4$)	ϵ_{ST} (%)	ϵ_{DT}^1 (%)	ϵ_{DT}^2 (%)	ϵ_{DT}^3 (%)	ϵ_{DT}^4 (%)	ϵ_{DT}^5 (%)	ϵ_{DT}^6 (%)	ϵ_{DT}^7 (%)
$\bar{D}^0 \to K^+\pi^-$	$(-27, 27)$	382.1 ± 0.2	66.67 ± 0.01	2.77 ± 0.04	2.84 ± 0.02	2.11 ± 0.02	4.56 ± 0.05	4.74 ± 0.05	3.29 ± 0.02	3.16 ± 0.03
$\bar{D}^0 \to K^+\pi^-\pi^0$	$(-62, 49)$	792.6 ± 0.3	37.92 ± 0.01	1.20 ± 0.03	1.42 ± 0.02	1.06 ± 0.02	2.46 ± 0.03	2.34 ± 0.03	1.97 ± 0.02	1.90 ± 0.02
$\bar{D}^0 \to K^+\pi^+\pi^-\pi^-$	$(-26, 24)$	514.0 ± 0.2	42.20 ± 0.01	1.25 ± 0.03	1.50 ± 0.02	1.15 ± 0.02	2.43 ± 0.03	2.33 ± 0.03	1.88 ± 0.02	1.81 ± 0.02

TABLE II. The $\Delta E_{\rm tag}$ requirements, ST yields ($N_{\rm ST}$), ST efficiencies ($\epsilon_{\rm ST}$) and DT efficiencies ($\epsilon_{\rm DT}$) for D^+ decays. The superscripts 8-10 identify the signal decays: ${}^8D^+ \to K^0_S K^0_S K^0_S \pi^+$, ${}^9D^+ \to K^0_S K^+ K^- \pi^+$ and ${}^{10}D^+ \to \phi K^0_S \pi^+$. The uncertainties are statistical only.

Tag mode	$\Delta E_{\rm tag}$ (MeV)	$N_{\rm ST}$ ($\times 10^4$)	$\epsilon_{\rm ST}$ (%)	$\epsilon^8_{\rm DT}$ (%)	$\epsilon^9_{\rm DT}$ (%)	$\epsilon^{10}_{\rm DT}$ (%)
$D^- \to K^+\pi^-\pi^-$	$(-25, 24)$	567.4 ± 0.2	52.40 ± 0.01	2.84 ± 0.04	2.78 ± 0.02	1.86 ± 0.02
$D^- \to K^0_S\pi^-$	$(-25, 26)$	66.7 ± 0.1	52.60 ± 0.01	2.88 ± 0.04	2.75 ± 0.02	1.81 ± 0.02
$D^- \to K^+\pi^-\pi^-\pi^0$	$(-57, 46)$	181.0 ± 0.2	25.62 ± 0.01	1.12 ± 0.03	1.17 ± 0.01	0.75 ± 0.01
$D^- \to K^0_S\pi^-\pi^0$	$(-62, 49)$	150.7 ± 0.1	27.74 ± 0.01	1.16 ± 0.03	1.39 ± 0.02	0.95 ± 0.02
$D^- \to K^0_S\pi^+\pi^-\pi^-$	$(-28, 27)$	81.0 ± 0.1	30.25 ± 0.01	1.02 ± 0.03	1.30 ± 0.01	0.86 ± 0.01
$D^- \to K^+K^-\pi^-$	$(-24, 23)$	49.2 ± 0.1	41.94 ± 0.01	2.25 ± 0.04	2.17 ± 0.02	1.42 ± 0.02

ST $\bar{D}^0$ and D^- yields in data and the corresponding ST efficiencies are summarized in the third and fourth columns of Tables I and II. The total yields of the ST $\bar{D}^0$ and D^- mesons in data are $(1688.7 \pm 0.5) \times 10^4$ and $(1096.0 \pm 0.4) \times 10^4$, respectively, where the uncertainties are statistical only.

VI. YIELDS OF DT EVENTS

Candidates for the signal decays $D^0 \to K^0_S K^0_S K^0_S \pi^0$, $D^0 \to K^0_S K^+ K^- \pi^0$, $D^0 \to K^0_S K^0_S K^- \pi^+$, $D^0 \to K^0_S K^0_S K^+ \pi^-$, $D^0 \to K^+ K^- K^- \pi^+$, $D^+ \to K^0_S K^0_S K^0_S \pi^+$, and $D^+ \to K^0_S K^+ K^- \pi^+$ are reconstructed from the remaining charged tracks and neutral showers that are not used in the

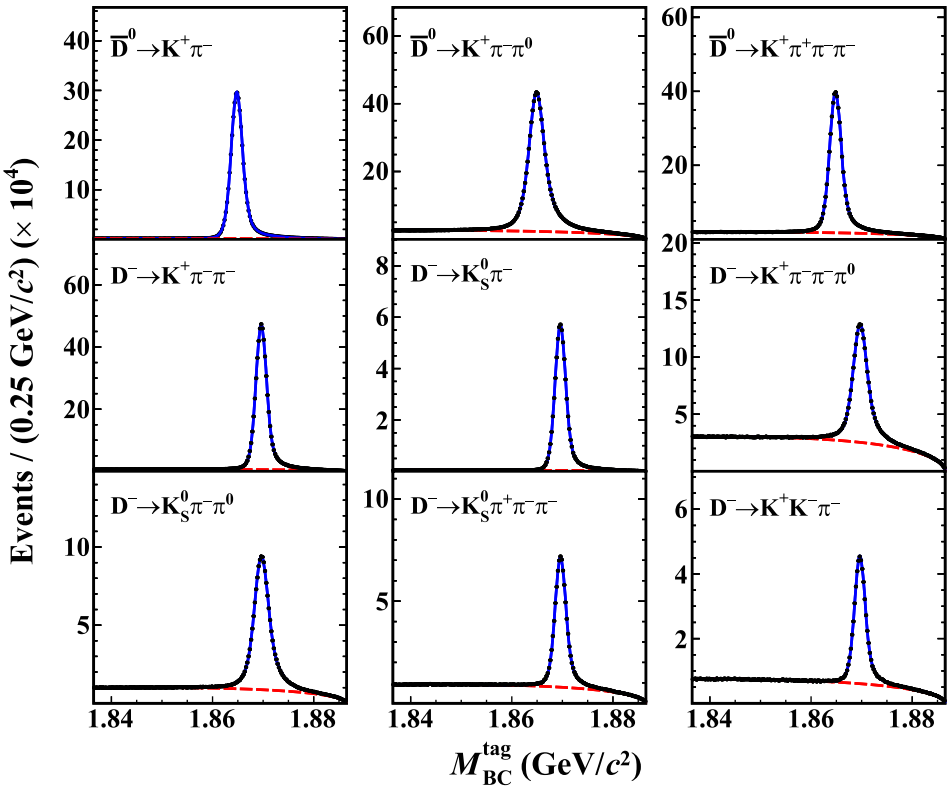


FIG. 1. Fits to the $M^{\rm tag}_{\rm BC}$ distributions of the ST $\bar{D}^0$ and D^- candidates. The dots with error bars show the data, the blue solid curves are the fit results and the red dotted lines are the fitted background shapes.

reconstruction of the ST $\bar{D}$ candidates. Due to good agreement between data and MC simulation, the uncertainty due to multiple candidates is negligible.

The signal D mesons are identified using the energy difference $\Delta E_{\rm sig}$ and the beam-constrained mass $M_{\rm BC}^{\rm sig}$, which are calculated with the "sig" analogs of the "tag" in Eqs. (4) and (5), respectively. For each signal mode, if there are multiple candidates in an event, only the one with the minimum $|\Delta E_{\rm sig}|$ is kept. The rates of multiple combinations for signal decays reconstructed exclusively with charged final-state particles are ranging between (2.2–10.2)%, and (28.9–52.5)% for decay modes containing π^0. Due to good agreement between data and MC simulation, the uncertainty due to multiple candidates is negligible. The signal decays are required to satisfy the mode-dependent $\Delta E_{\rm sig}$ requirements, as shown in the second column of Table III.

The yield of each signal decay ($N_{\rm DT}^{\rm fit}$) is obtained from an unbinned maximum-likelihood fit to the $M_{\rm BC}^{\rm sig}$ distribution of the selected DT candidates. In the fit, the signal shape is modeled by an MC-simulated shape convolved with a Gaussian function, while the combinatorial background is described by an ARGUS function [28],

$$\begin{aligned}\mathrm{ARGUS}(m, m_0, c, p) = \mathcal{N}\cdot m\cdot\left[1-\left(\frac{m}{m_0}\right)^2\right]^p \\ \cdot\exp\left[c\cdot\left(1-\left(\frac{m}{m_0}\right)^2\right)\right].\end{aligned} \quad (6)$$

Here, the parameters of the convolved Gaussian resolution function and the ARGUS function are free, except for the m_0, which is set to be $E_{\rm beam}/2 = 1.8865\ \mathrm{GeV}/c^2$. The signal decays involving a K_S^0 in the final state suffer from nonresonant $\pi^+\pi^-$ background surviving the K_S^0 selection criteria. Such background events may form peaking backgrounds around the nominal D^0 or D^+ mass in the $M_{\rm BC}^{\rm sig}$ distributions. This background contribution is estimated with events in the K_S^0 sideband region of $0.020\ \mathrm{GeV}/c^2 < |M_{\pi^+\pi^-} - 0.498\ \mathrm{GeV}/c^2| < 0.044\ \mathrm{GeV}/c^2$. No significant peaking background is observed in any signal decay, thus this background is neglected in the baseline measurements, but treated as a source of systematic uncertainty. The resulting fits for the seven inclusive decays are shown in Fig. 2. For each signal decay, the statistical significance is greater than 5σ, which is calculated as $\sqrt{2\times(\ln\mathcal{L}_{\rm sig} - \ln\mathcal{L}_0)}$, where $\ln\mathcal{L}_{\rm sig}$ and $\ln\mathcal{L}_0$ are the natural logarithm of likelihoods with and without the signal component in the fit [29]. The obtained fitted signal yields of $D\to KKK\pi$ decays and their statistical significance are listed in the third and fourth columns of Table III.

We note that only peaking contributions could bias the double-tag signal yield; smooth combinatorial backgrounds are absorbed by the fit. These contributions include both peaking backgrounds on the signal side and events where a true signal decay on one side is accompanied by a combinatorial candidate on the other side that satisfies the single-tag requirements. Such contributions are strongly suppressed by the double-tag selection. Using an inclusive

TABLE III. Requirements on $\Delta E_{\rm sig}$, fitted signal yields in data ($N_{\rm DT}$), signal efficiencies which include the branching fractions of the subdecays $K_S^0\to\pi^+\pi^-$, $\pi^0\to\gamma\gamma$ ($\epsilon_{\rm sig}$), statistical significance ($\mathcal{S}$), the obtained branching fractions $\mathcal{B}_{\rm sig}$ ($\times10^{-5}$) and relative branching fractions of $D\to\phi K\pi$ to $D\to KKK\pi$ $\mathcal{B}_{\rm relative}$ (%) for the different signal decays. The first and second uncertainties for $\mathcal{B}_{\rm sig}$ are statistical and systematic, respectively, while the uncertainties for $N_{\rm DT}$ and $\epsilon_{\rm sig}$ are statistical only. For comparison, the relevant PDG branching fractions $\mathcal{B}_{\rm PDG}$ ($\times10^{-5}$) and relative branching fractions $\mathcal{B}_{\rm relative}^{\rm PDG}$ (%) are listed in the last column.

Signal mode	$\Delta E_{\rm sig}$ (MeV)	$N_{\rm DT}$	$\mathcal{S}(\sigma)$	$\epsilon_{\rm sig}$ (%)	$\mathcal{B}_{\rm sig}$	$\mathcal{B}_{\rm relative}$	$\mathcal{B}_{\rm PDG}$ [4]	$\mathcal{B}_{\rm relative}^{\rm PDG}$ [4]
$D^0\to K_S^0K_S^0K_S^0\pi^0$	$(-26, 22)$	$14.5^{+4.2}_{-3.6}$	6.9	1.10 ± 0.02	$7.8^{+2.3}_{-2.0}\pm1.5$	⋯	⋯	⋯
$D^0\to K_S^0K^+K^-\pi^0$	$(-27, 23)$	$81.0^{+11.3}_{-10.7}$	>10	2.60 ± 0.02	$18.4^{+2.6}_{-2.5}\pm2.4$	⋯	⋯	⋯
$D^0\to\phi K_S^0\pi^0$	$(-27, 23)$	$36.8^{+8.7}_{-8.1}$	6.4	1.96 ± 0.03	⋯	$61^{+15}_{-14}\pm10$	⋯	⋯
$D^0\to K_S^0K_S^0K^-\pi^+$	$(-20, 19)$	$66.2^{+8.6}_{-7.9}$	>10	3.04 ± 0.04	$12.9^{+1.7}_{-1.6}\pm1.3$	⋯	59.0 ± 13.0	⋯
$D^0\to K_S^0K_S^0K^+\pi^-$	$(-20, 19)$	$28.7^{+5.9}_{-5.3}$	8.7	2.96 ± 0.04	$5.7^{+1.2}_{-1.1}\pm1.0$	⋯		
$D^0\to K^+K^-K^-\pi^+$	$(-21, 19)$	$144.3^{+14.2}_{-13.5}$	>10	4.91 ± 0.04	$17.4^{+1.8}_{-1.7}\pm2.2$	⋯	22.5 ± 3.2	⋯
$D^0\to\phi K^-\pi^+$	$(-21, 19)$	$98.8^{+13.5}_{-12.7}$	>10	4.73 ± 0.02	⋯	$71^{+10}_{-10}\pm13$	⋯	65.8 ± 11.7
$D^+\to K_S^0K_S^0K_S^0\pi^+$	$(-21, 20)$	$10.8^{+3.7}_{-3.0}$	6.4	1.63 ± 0.02	$6.0^{+2.1}_{-1.7}\pm1.6$	⋯	⋯	⋯
$D^+\to K_S^0K^+K^-\pi^+$	$(-21, 20)$	$52.9^{+9.0}_{-8.2}$	9.9	3.50 ± 0.02	$13.8^{+2.4}_{-2.2}\pm2.5$	⋯	24.0 ± 5.0	⋯
$D^+\to\phi K_S^0\pi^+$	$(-21, 20)$	$20.6^{+7.5}_{-6.6}$	5.0	2.33 ± 0.02	⋯	$59^{+22}_{-19}\pm9$	⋯	⋯

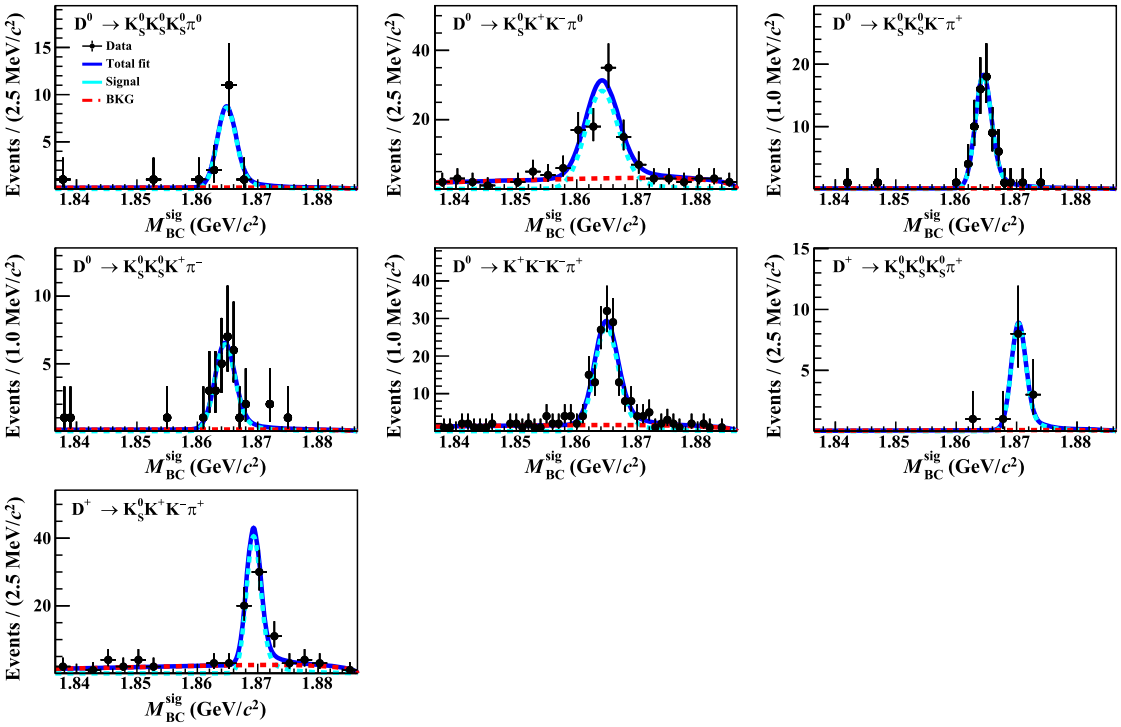


FIG. 2. Fits to the $M_{\rm BC}^{\rm sig}$ distributions of the DT candidates for $D^0 \to K_S^0 K_S^0 K_S^0 \pi^0$, $D^0 \to K_S^0 K^+ K^- \pi^0$, $D^0 \to K_S^0 K_S^0 K^- \pi^+$, $D^0 \to K_S^0 K_S^0 K^+ \pi^-$, $D^0 \to K^+ K^- K^- \pi^+$, $D^+ \to K_S^0 K_S^0 K_S^0 \pi^+$, and $D^+ \to K_S^0 K^+ K^- \pi^+$. The dots with error bars are data, the blue solid curves are the total fit shapes, the cyan dashed curves show fits to the signal shapes and the red dashed curves fits to the background shapes.

MC sample of $\psi(3770)$ with 40 times the data luminosity, and applying truth matching to both the D and $\bar{D}$ candidates, the residual peaking contribution, after scaling to our measured branching fractions, is below 2% and thus negligible.

We further examine the $M_{K^+K^-}$ distributions of the accepted DT candidates for $D^0 \to K_S^0 K^+ K^- \pi^0$, $D^0 \to K^+ K^- K^- \pi^+$, and $D^+ \to K_S^0 K^+ K^- \pi^+$, and significant ϕ signals are found. To determine the signal yield of each $D \to \phi K \pi$ decay, we perform a two-dimensional unbinned maximum-likelihood fit to the $M_{K^+K^-}$ versus $M_{\rm BC}^{\rm sig}$ distribution. In the fit, the ϕ signal is described by a Breit-Wigner (BW) function convolved with a Gaussian function, while the combinatorial K^+K^- background is described by a reversed ARGUS function, i.e., an ARGUS function where the independent variable m is replaced

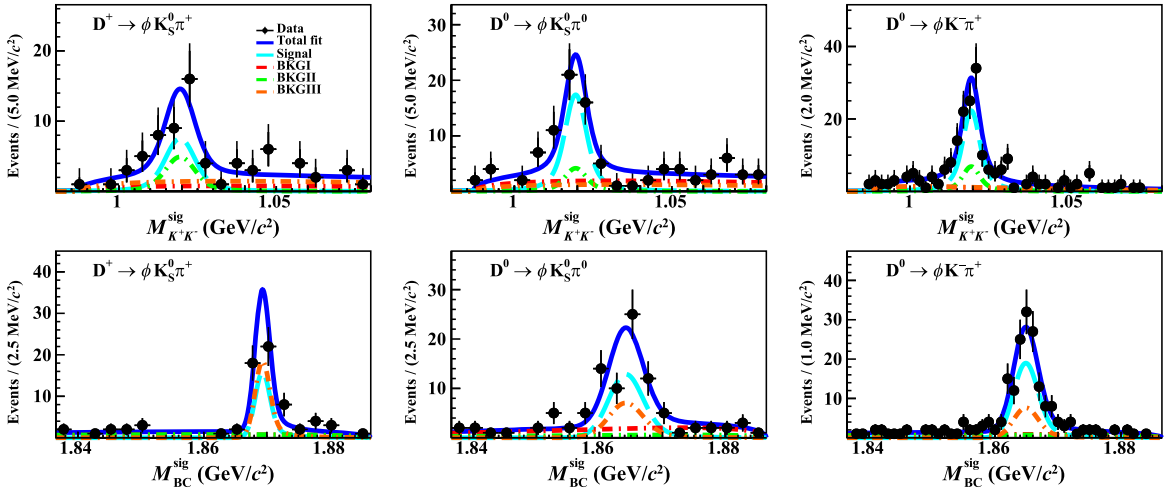


FIG. 3. Fits to the $M_{\rm BC}^{\rm sig}$ versus $M_{K^+K^-}^{\rm sig}$ distributions of DT events for $D^0 \to \phi K_S^0 \pi^0$, $D^0 \to \phi K^- \pi^+$, and $D^+ \to \phi K_S^0 \pi^+$. The dots with error bars are data, cyan dashed curves are fit signal, red dashed curves are fit BKGI, green dashed curves are fit BKGII and the orange dashed curves are fit BKGIII.

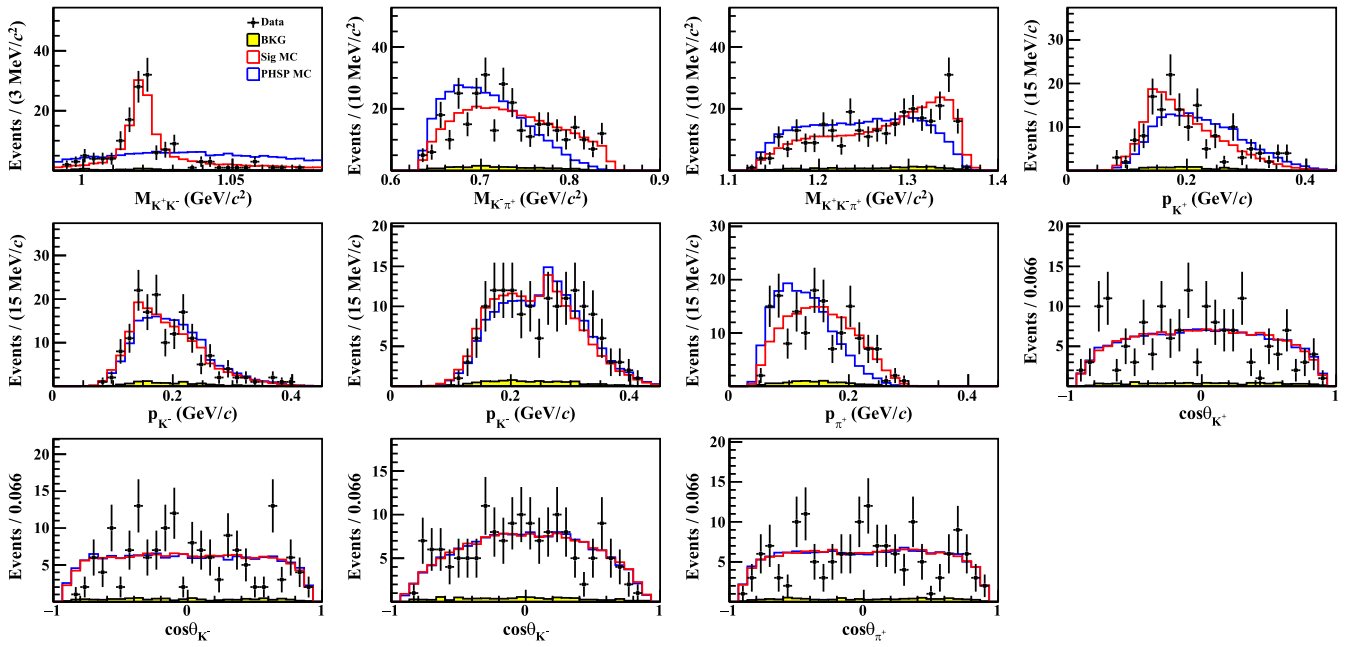


FIG. 4. Distributions of the momenta and cosines of polar angles of the daughter particles as well as the invariant masses of two-body and three-body combinations of the $D^0 \to K^+K^-K^-\pi^+$ candidates, comparing data (dots with error bars) and the signal MC samples (red and blue histograms). The red histogram shows the mixed signal MC sample and the blue one the PHSP MC. The yellow filled histograms represent the MC-simulated backgrounds (BKG) from the inclusive MC sample.

by $2m_0 - m$, and m_0 in the $M_{K^+K^-}$ fit is set to be 0.987 GeV/c^2, which is the K^+K^- mass production threshold [4]. The mass and width of ϕ are fixed to their PDG values and the other parameters are allowed to float. There are four components in the two-dimensional fit. The first is the signal part ($S_{M_{\rm BC}^{\rm sig}} \cdot S_{M_{K^+K^-}}$), the second is BKGI ($S_{M_{\rm BC}^{\rm sig}} \cdot B_{M_{K^+K^-}}$), the third is BKGII ($B_{M_{\rm BC}^{\rm sig}} \cdot S_{M_{K^+K^-}}$), the last is BKGIII ($B_{M_{\rm BC}^{\rm sig}} \cdot B_{M_{K^+K^-}}$), where $S_{M_{\rm BC}^{\rm sig}}$ is the MC shape $(M_{\rm BC}^{\rm sig}) \otimes$ Gaussian ($\otimes$ represents convolution), $S_{M_{K^+K^-}}$ is BW $\otimes$ Gaussian, $B_{M_{\rm BC}^{\rm sig}}$ is an ARGUS function and $B_{M_{K^+K^-}}$ is a reversed ARGUS function. The fit results for these three decays are shown in Fig. 3. The same method as above is also used to evaluate the statistical significance of each $D \to \phi K\pi$ decay. The fitted signal yields of $D \to \phi K\pi$ decays and their statistical significance are also listed in the third and fourth columns of Table III.

The DT efficiencies are determined from MC simulation, and are summarized in Tables I and II, respectively, and the resulting signal efficiencies averaged over tag modes are summarized in the fifth column of Table III. As an example, Fig. 4 shows the distributions of the momenta and cosines of the polar angles of the daughter particles as well as the invariant masses of two-body or three-body particle combinations of the candidates for $D^0 \to K^+K^-K^-\pi^+$ between data and MC simulation. The comparisons for other $D \to KKK\pi$ decays can be found in the Appendix.

The obtained branching fractions and relative branching fractions of each signal decay are summarized in the sixth and the seventh column of Table III.

VII. SYSTEMATIC UNCERTAINTIES

The systematic uncertainties are estimated relative to the measured branching fractions and discussed below. Benefiting from the DT method, the systematic uncertainties related to the tag selection cancel.

The systematic uncertainties in the total yields of ST $\bar{D}$ mesons, which are mainly due to the fits to the $M_{\rm BC}$ distributions of the ST $\bar{D}$ candidates, were previously estimated to be 0.3% for ST $\bar{D}^0$ and D^- [26].

The tracking and PID efficiencies of charged particles are studied with control samples from the DT candidates of $D^0 \to K^-\pi^+$, $K^-\pi^+\pi^0$, $K^-\pi^-\pi^+\pi^+$ versus $\bar{D}^0 \to K^+\pi^-$, $K^+\pi^-\pi^0$, $K^+\pi^+\pi^-\pi^-$, as well as $D^+ \to K^-\pi^+\pi^+$ versus $D^- \to K^+\pi^-\pi^-$, which will miss a $\pi^\pm$ or $K^\pm$. The systematic uncertainties of tracking and PID are assigned as 0.5% per $K^\pm$ or $\pi^\pm$.

The systematic uncertainty in K_S^0 reconstruction is estimated using control samples of $J/\psi \to K^*(892)^\mp K^\pm$ and $J/\psi \to \phi K_S^0 K^\pm \pi^\mp$ [30] and found to be 1.5% per K_S^0. The systematic uncertainty of π^0 reconstruction is assigned as 3.0% per π^0 with the control sample of $D^0 \to K^-\pi^+\pi^0$ versus $\bar{D}^0 \to K^+\pi^-$ and $\bar{D}^0 \to K^+\pi^+\pi^-\pi^-$ [26].

The uncertainties of the quoted branching fractions of $\pi^0 \to \gamma\gamma$, $K^0_S \to \pi^+\pi^-$, and $\phi \to K^+K^-$ are 0.03%, 0.07%, and 1.0%, respectively [4].

The systematic uncertainties due to difference between data and MC in the $\Delta E_{\rm sig}$ requirements are studied using the DT events $D^0 \to K^0_S K^0_S \pi^0 \pi^0$, $D^0 \to K^0_S K^- \pi^+ \pi^0$, $D^0 \to K^0_S K^0_S \pi^+ \pi^-$, $D^0 \to K^+ K^- \pi^+ \pi^-$, $D^+ \to K^0_S K^+ \pi^+ \pi^-$, and $D^+ \to K^0_S K^0_S \pi^+ \pi^0$ versus the same $\bar{D}$ tags as in the baseline analysis. The efficiency differences between data and MC simulation, (0.6–5.9)%, are assigned as the systematic uncertainties for various signal decays.

The systematic uncertainty in the fit to the $M^{\rm sig}_{\rm BC}$ distribution is evaluated by changing the signal and background parametrizations. Specifically, the signal shape is replaced with a version that excludes Gaussian smearing and the endpoint of the ARGUS function is varied by ± 0.2 MeV/c^2 [31]. To estimate the uncertainty due to the $M_{K^+K^-}$ fit, the alternative signal shape is obtained by replacing the original shape with the MC shape and the uncertainty of the background shape is obtained by varying the endpoint of the inverse-ARGUS function (± 0.2 MeV/c^2). The relative changes of the signal shape and background shape are assigned as individual systematic uncertainties. Adding these two effects in quadrature results in systematic uncertainties of (1.4–10.0)%.

The systematic uncertainty associated with nonresonant $\pi^+\pi^-$ pairs misidentified as K^0_S mesons is evaluated by comparing the fitted signal yields with and without including this background component.

The uncertainties due to limited size of the MC sample are assigned by $\frac{1}{\sqrt{N}}\sqrt{\frac{1-\epsilon}{\epsilon}}$, where ϵ is the detection efficiency and N is the total number of produced signal MC events. The systematic uncertainties are (1.0–1.8)%, depending on the signal decay.

The imperfect simulations of the momentum and $\cos\theta$ distributions of charged particles in signal decays are considered as a source of systematic uncertainty named MC generator. For decays with ϕ components, the systematic uncertainty is evaluated by varying the input branching fractions of the known ϕ decays within $\pm 1\sigma$ of their fitted ratios. For decays without a clear intermediate resonance, the systematic uncertainty is taken as the maximum difference between the nominal signal MC sample and the alternative signal MC sample reweighted to the data distribution. The relative resulting changes in signal efficiencies, (4.6–23.8)%, are taken as the systematic uncertainties.

The QC effect should be corrected by a factor $f_{\rm QC} = \frac{1}{1-C_f(2f_{CP+}-1)}$ as described in Ref. [25]. Due to the low signal yields, we do not apply QC correction in this analysis, but consider it as one of the sources of systematic uncertainty. For all D^0 signal decays, a conservative uncertainty, 7.0%, due to QC effects is assigned as the systematic uncertainty [32,33].

The systematic uncertainty due to the tag bias, arising from differences in the single-tag D^0 and D^+ reconstruction environment between generic and signal events, is evaluated following the method of Ref. [34]. Potential simulation imperfections in tracking, particle identification, π^0, and K^0_S reconstruction are studied, and their effect on the tag efficiency ratio is taken as the corresponding uncertainty. The resulting systematic uncertainties are (0.2–0.5)% depending on the signal decay.

TABLE IV. Relative systematic uncertainties (%) in the measurements of the branching fractions of ${}^1D^0 \to K^0_S K^0_S K^0_S \pi^0$, ${}^2D^0 \to K^0_S K^+ K^- \pi^0$, ${}^3D^0 \to \phi K^0_S \pi^0$, ${}^4D^0 \to K^0_S K^0_S K^- \pi^+$, ${}^5D^0 \to K^0_S K^0_S K^+ \pi^-$, ${}^6D^0 \to K^+ K^- K^- \pi^+$, ${}^7D^0 \to \phi K^- \pi^+$, ${}^8D^+ \to K^0_S K^0_S K^0_S \pi^+$, ${}^9D^+ \to K^0_S K^+ K^- \pi^+$, and ${}^{10}D^+ \to \phi K^0_S \pi^+$.

	D^0							D^+		
Source	1	2	3	4	5	6	7	8	9	10
$N^{\rm tot}_{\rm ST}$	0.3	0.3	···	0.3	0.3	0.3	···	0.3	0.3	···
$\pi^\pm/K^\pm$ tracking	3.0	2.0	···	3.0	3.0	2.0	···	3.5	2.5	···
$\pi^\pm/K^\pm$ PID	···	1.0	···	1.0	1.0	2.0	···	0.5	1.5	···
K^0_S reconstruction	4.5	1.5	···	3.0	3.0	···	···	4.5	1.5	···
π^0 reconstruction	3.0	3.0	···	···	···	···	···	···	···	···
K^0_S/π^0 $\mathcal{B}$	0.3	0.1	1.0	0.2	0.2	···	1.0	0.3	0.1	1.0
$\Delta E_{\rm sig}$ cut	5.9	0.8	···	0.6	0.6	3.5	···	0.6	3.1	···
DT fit background	4.3	1.5	3.4	1.9	1.4	4.7	8.4	6.6	8.9	10.0
K^0_S nonresonant background	2.4	2.1	2.1	1.5	0.0	···	···	5.2	1.5	1.5
Limited MC samples	1.8	1.1	1.1	1.0	1.0	1.0	1.0	1.2	1.1	1.1
MC generator	14.9	9.5	13.0	4.6	14.5	8.1	13.6	23.8	14.3	10.9
QC effect	7.0	7.0	7.0	7.0	7.0	7.0	7.0	···	···	···
Tag bias	0.4	0.2	0.2	0.4	0.2	0.2	0.2	0.5	0.3	0.3
Total	19.3	12.9	15.4	9.9	16.8	12.6	17.6	25.9	17.6	15.0

Table IV summarizes the systematic uncertainties in the branching fraction measurements. For the decays containing ϕ, relative branching fractions are reported, such that the uncertainties due to $N_{\rm ST}^{\rm tot}$, $\pi^{\pm}/K^{\pm}$ tracking and PID, K_S^0 and π^0 reconstruction, and $\Delta E_{\rm sig}$ of relative branching fractions of $D \to \phi K\pi$ cancel out in the ratio. For each signal decay, the total systematic uncertainty is obtained by adding all individual contributions in quadrature. The obtained total systematic uncertainties range between (9.9–25.9)% for different signal decays.

VIII. SUMMARY

By analyzing 20.3 fb^{-1} of e^+e^- collision data taken at $\sqrt{s} = 3.773$ GeV with the BESIII detector, we determine the branching fractions of the hadronic decays $D^0 \to K_S^0K_S^0K_S^0\pi^0$, $D^0 \to K_S^0K^+K^-\pi^0$, $D^0 \to K_S^0K_S^0K^-\pi^+$, $D^0 \to K_S^0K_S^0K^+\pi^-$, $D^0 \to K^+K^-K^-\pi^+$, $D^+ \to K_S^0K_S^0K_S^0\pi^+$, and $D^+ \to K_S^0K^+K^-\pi^+$. The decays $D^0 \to \phi K_S^0\pi^0$, $D^0 \to \phi K^-\pi^+$, and $D^+ \to \phi K_S^0\pi^+$ are found to be the main subprocesses in $D^0 \to K_S^0K^+K^-\pi^0$, $D^0 \to K^+K^-K^-\pi^+$, and $D^+ \to K_S^0K^+K^-\pi^+$, respectively; and their relative branching fractions to $\mathcal{B}(D \to KKK\pi)$ are determined. The systematic uncertainties associated with $K^{\pm}/\pi^{\pm}$ tracking and PID as well as K_S^0 and π^0 reconstruction are partially correlated with those in previous BESIII measurements [35]. All the obtained results are shown in Table III.

The branching fractions of $D^0 \to K_S^0K_S^0K_S^0\pi^0$, $D^0 \to K_S^0K^+K^-\pi^0$, $D^0 \to \phi K_S^0\pi^0$, $D^+ \to K_S^0K_S^0K_S^0\pi^+$, and $D^+ \to \phi K_S^0\pi^+$ are measured for the first time; and those of $D^0 \to K_S^0K_S^0K^-\pi^+$, $D^0 \to K_S^0K_S^0K^+\pi^-$, $D^0 \to K^+K^-K^-\pi^+$, $D^0 \to \phi K^-\pi^+$, and $D^+ \to K_S^0K^+K^-\pi^+$ are measured with improved precision. Our branching fractions of $D^0 \to K^+K^-K^-\pi^+$ and $D^+ \to K_S^0K^+K^-\pi^+$ are consistent with the respective PDG values [4] within 1.2σ and 1.7σ, respectively. The summed branching fraction of $D^0 \to K_S^0K_S^0K^-\pi^+$ and $D^0 \to K_S^0K_S^0K^+\pi^-$ presented in this work deviates from the combined branching fraction of $D^0 \to K_S^0K_S^0K^{\pm}\pi^{\mp}$ based on the FOCUS measurement [7] by 3.0σ.

ACKNOWLEDGMENTS

The BESIII Collaboration thanks the staff of BEPCII [36] and the IHEP computing center for their strong support. This work is supported in part by National Key R&D Program of China under Contracts No. 2023YFA1606000, No. 2023YFA1606704; National Natural Science Foundation of China (NSFC) under Contracts No. 12675104, No. 11635010, No. 11935015, No. 11935016, No. 11935018, No. 12025502, No. 12035009, No. 12035013, No. 12061131003, No. 12192260, No. 12192261, No. 12192262, No. 12192263, No. 12192264, No. 12192265, No. 12221005, No. 12225509, No. 12235017, No. 12361141819; the Chinese Academy of Sciences (CAS) Large-Scale Scientific Facility Program; CAS under Contract No. YSBR-101; 100 Talents Program of CAS; The Institute of Nuclear and Particle Physics (INPAC) and Shanghai Key Laboratory for Particle Physics and Cosmology; the Fundamental Research Funds for the Central Universities under Contract No. 010-63263110; ERC under Contract No. 758462; German Research Foundation DFG under Contract No. FOR5327; Istituto Nazionale di Fisica Nucleare, Italy; Knut and Alice Wallenberg Foundation under Contracts No. 2021.0174, No. 2021.0299; Ministry of Development of Turkey under Contract No. DPT2006K-120470; National Research Foundation of Korea under Contract No. NRF-2022R1A2C1092335; National Science and Technology fund of Mongolia; Polish National Science Centre under Contract No. 2024/53/B/ST2/00975; STFC (United Kingdom); Swedish Research Council under Contract No. 2019.04595; U.S. Department of Energy under Contract No. DE-FG02-05ER41374.

DATA AVAILABILITY

There are no publicly available research data or software supporting this manuscript. Requests for further information or data should be sent to the authors.

APPENDIX

Figures 5–10 show the comparisons of the distributions of the momenta and cosines of the polar angles of the daughter particles, as well as the invariant masses of two-body or three-body particle combinations of the candidates for $D^0 \to K_S^0K_S^0K_S^0\pi^0$, $D^0 \to K_S^0K^+K^-\pi^0$, $D^0 \to K_S^0K_S^0K^-\pi^+$, $D^0 \to K_S^0K_S^0K^+\pi^-$, $D^+ \to K_S^0K_S^0K_S^0\pi^+$, and $D^+ \to K_S^0K^+K^-\pi^+$ between data and MC simulation, respectively.

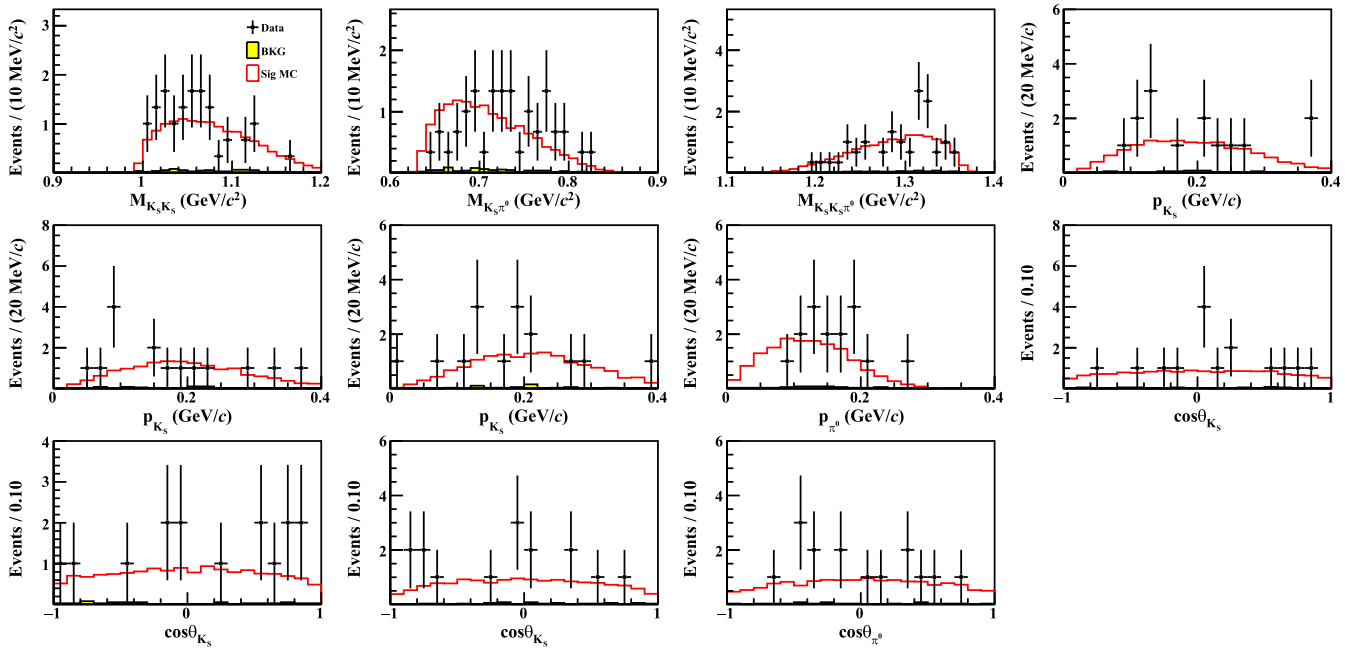


FIG. 5. Comparisons of some typical distributions for the $D^0 \to K^0_S K^0_S K^0_S \pi^0$ candidate events between data (dots with error bars) and the PHSP signal MC sample (red histograms). The yellow filled histograms represent the MC-simulated BKG from the inclusive MC sample. The final state contains three identical particles K^0_S. The distributions include the invariant-mass combinations of the $K^0_S\pi^0$, $K^0_S K^0_S$ and $K^0_S K^0_S \pi^0$ systems, each scaled by $1/3$ to keep the total number of entries in each distribution identical to the number of candidate events.

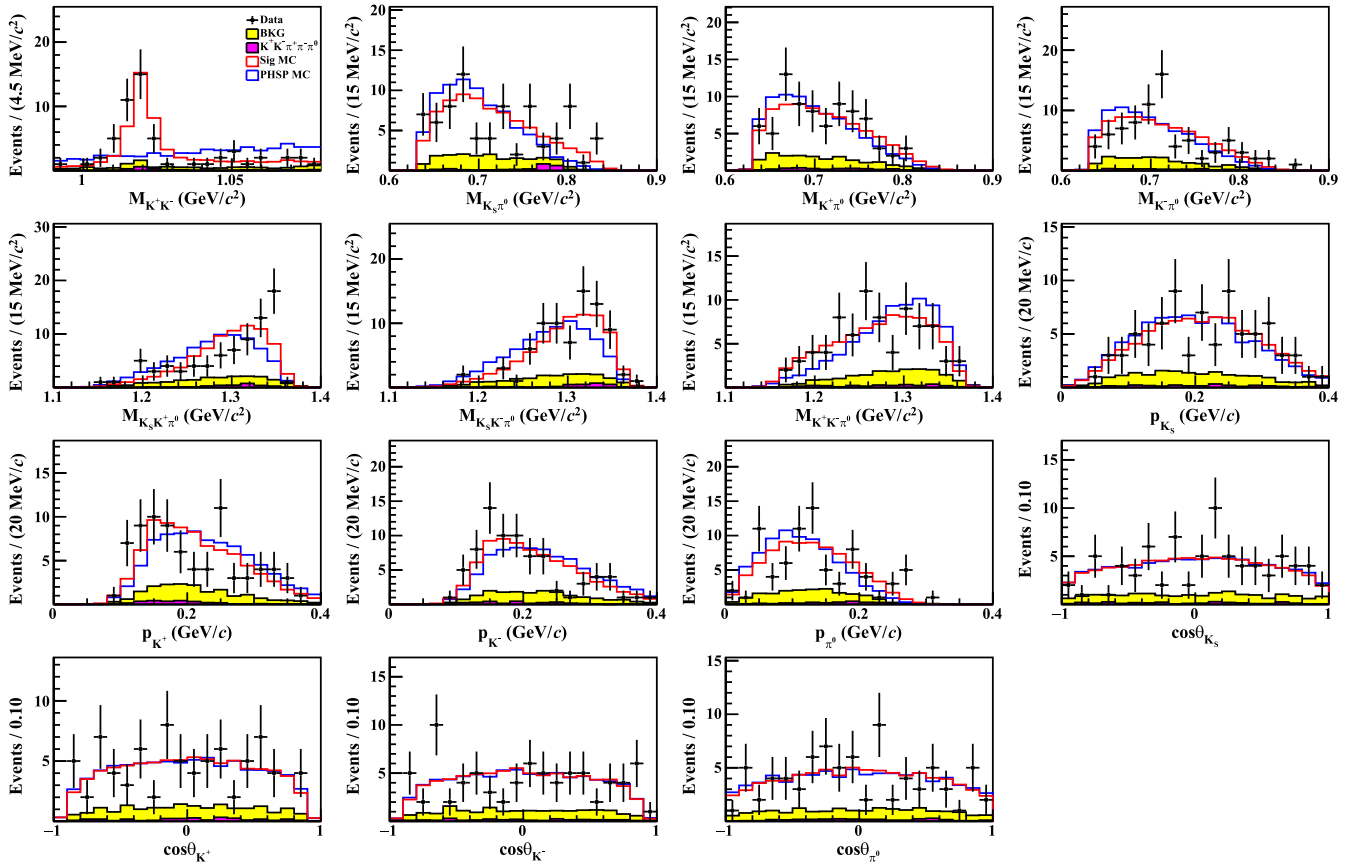


FIG. 6. Comparisons of some typical distributions for the $D^0 \to K^0_S K^+ K^- \pi^0$ candidate events between data (dots with error bars) and the signal MC sample (red and blue histograms), where the red one shows the mixed signal MC sample and the blue one the PHSP MC. The yellow filled histograms represent the MC-simulated BKG from the inclusive MC sample.

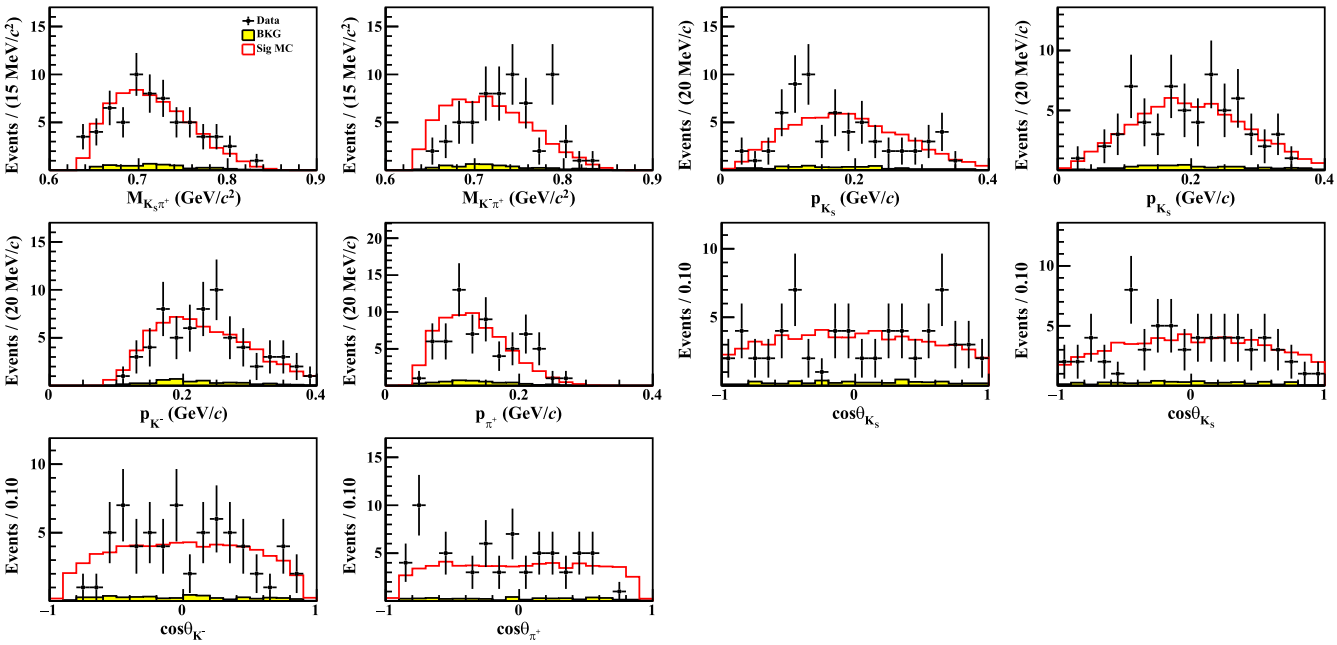


FIG. 7. Comparisons of some typical distributions for the $D^0 \to K^0_S K^0_S K^- \pi^+$ candidate events between data (dots with error bars) and the PHSP signal MC sample (red histograms). The yellow filled histograms represent the MC-simulated BKG from the inclusive MC sample. The distributions of invariant-mass combinations of the $K^0_S \pi^+$ is scaled by $1/2$ to keep the total number of entries in each distribution identical to the number of candidate events.

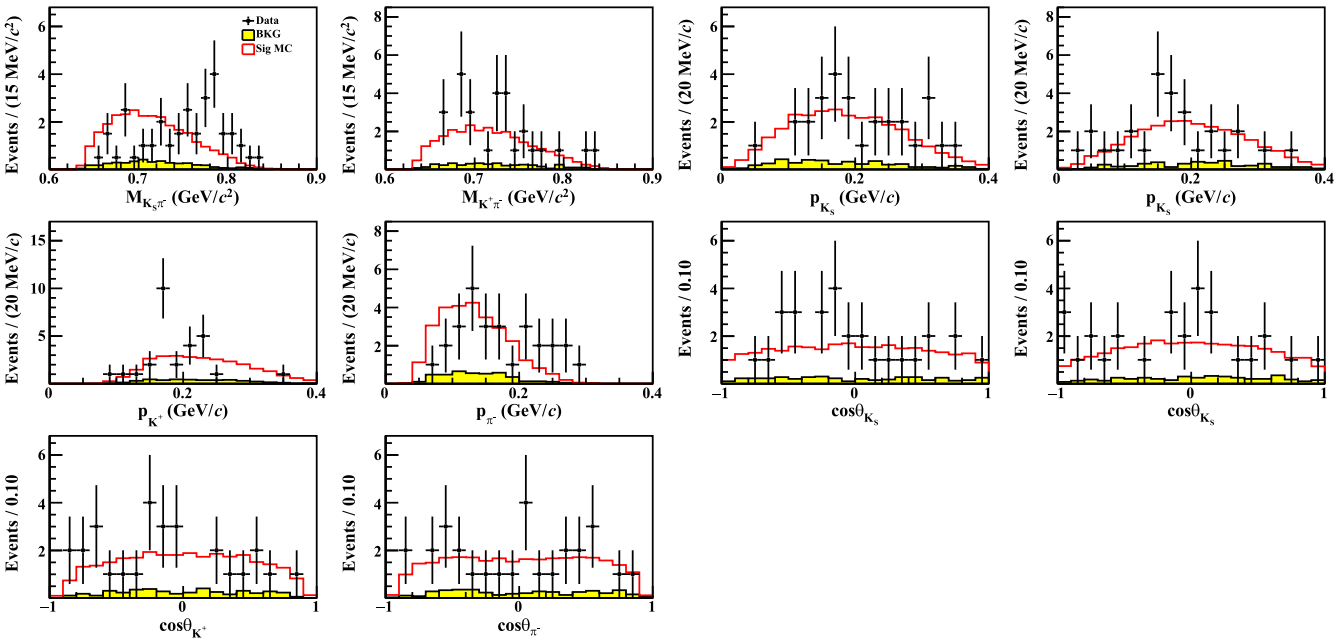


FIG. 8. Comparisons of some typical distributions for the $D^0 \to K^0_S K^0_S K^+ \pi^-$ candidate events between data (dots with error bars) and the PHSP signal MC sample (red histograms). The yellow filled histograms represent the MC-simulated BKG from the inclusive MC sample. The final state contains two identical particles K^0_S. The distributions of invariant-mass combinations of the $K^0_S \pi^-$ is scaled by $1/2$ to keep the total number of entries in each distribution identical to the number of candidate events.

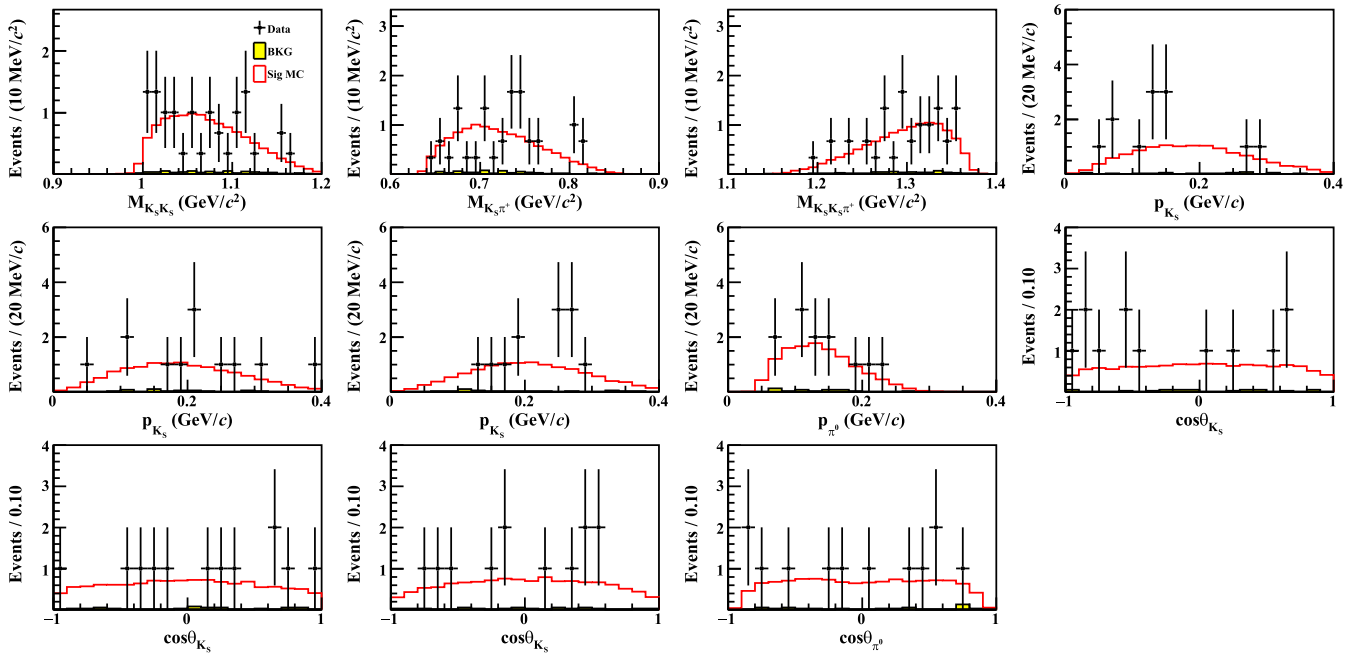


FIG. 9. Comparisons of some typical distributions for the $D^+ \to K^0_S K^0_S K^0_S \pi^+$ candidate events between data (dots with error bars) and the PHSP signal MC sample (red histograms). The yellow filled histograms represent the MC-simulated BKG from the inclusive MC sample. The final state contains three identical particles K^0_S. The distributions include the invariant-mass combinations of the $K^0_S K^0_S$, $K^0_S \pi^+$, and $K^0_S K^0_S \pi^+$ systems, each scaled by $1/3$ to keep the total number of entries in each distribution identical to the number of candidate events.

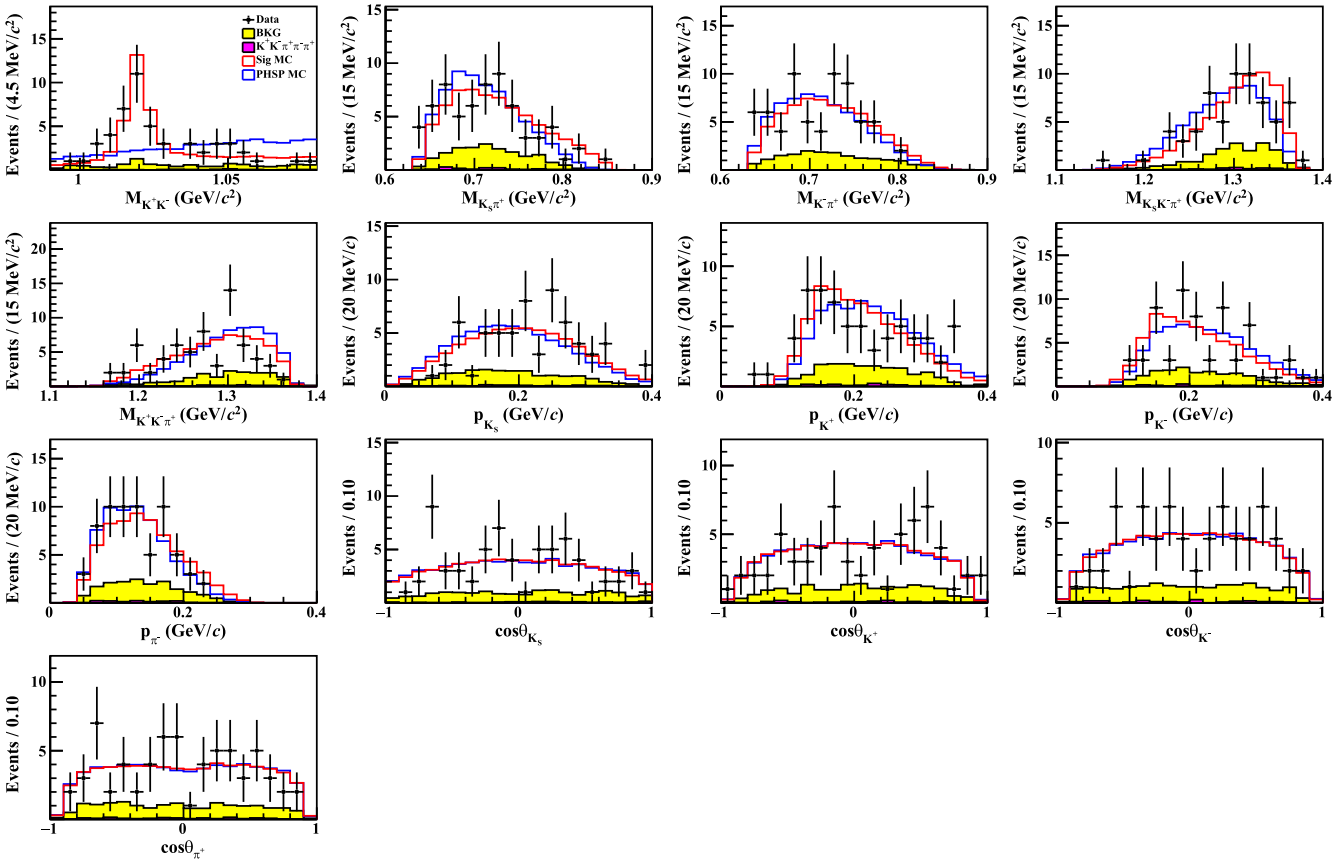


FIG. 10. Comparisons of some typical distributions for the $D^+ \to K^0_S K^+ K^- \pi^+$ candidate events between data (dots with error bars) and the signal MC sample (red and blue histograms), where the red one shows the mixed signal MC sample and the blue one the PHSP MC. The yellow filled histograms represent the MC-simulated BKG from the inclusive MC sample.

[1] H.-Y. Cheng, Chin. J. Phys. **34**, 855 (1996), https://www.airitilibrary.com/Article/Detail/05779073-199606-201211280001-201211280001-855-861.

[2] Y. Fu-Sheng, X.-X. Wang, and C.-D. Lu, Phys. Rev. D **84**, 074019 (2011).

[3] H. J. Lipkin, Phys. Rev. Lett. **44**, 710 (1980).

[4] S. Navas *et al.* (Particle Data Group), Phys. Rev. D **110**, 030001 (2024).

[5] J. M. Link *et al.* (FOCUS Collaboration), Phys. Lett. B **575**, 190 (2003).

[6] J. M. Link *et al.* (FOCUS Collaboration), Phys. Rev. Lett. **87**, 162001 (2001).

[7] J. M. Link *et al.* (FOCUS Collaboration), Phys. Lett. B **607**, 59 (2005).

[8] M. Ablikim *et al.* (BESIII Collaboration), Chin. Phys. C **48**, 123001 (2024).

[9] M. Ablikim *et al.* (BESIII Collaboration), Nucl. Instrum. Methods Phys. Res., Sect. A **614**, 345 (2010).

[10] C. Yu *et al.*, in *7th International Particle Accelerator Conference* (JACoW, 2016), pp. 1014–1018, 10.18429/JACoW-IPAC2016-TUYA01.

[11] X. Li *et al.*, Radiat. Detect. Technol. Methods **1**, 13 (2017).

[12] Y. X. Guo *et al.*, Radiat. Detect. Technol. Methods **1**, 15 (2017).

[13] P. Cao *et al.*, Nucl. Instrum. Methods Phys. Res., Sect. A **953**, 163053 (2020).

[14] S. Agostinelli *et al.* (GEANT4 Collaboration), Nucl. Instrum. Methods Phys. Res., Sect. A **506**, 250 (2003).

[15] S. Jadach, B. Ward, and Z. Was, Comput. Phys. Commun. **130**, 260 (2000).

[16] D. J. Lange, Nucl. Instrum. Methods Phys. Res., Sect. A **462**, 152 (2001).

[17] R. G. Ping, Chin. Phys. C **32**, 599 (2008).

[18] M. Ablikim *et al.* (BESIII Collaboration), Phys. Rev. D **95**, 072010 (2017).

[19] M. Ablikim *et al.* (BESIII Collaboration), J. High Energy Phys. 05 (2025) 195.
[20] M. Ablikim *et al.* (BESIII Collaboration), Phys. Rev. D **89**, 052001 (2014).
[21] J. C. Chen, G. S. Huang, X. R. Qi, D. H. Zhang, and Y. S. Zhu, Phys. Rev. D **62**, 034003 (2000).
[22] R. L. Yang, R. G. Ping, and H. Chen, Chin. Phys. Lett. **31**, 061301 (2014).
[23] N. Davidson, T. Przedzinski, and Z. Was, Comput. Phys. Commun. **199**, 86 (2016).
[24] R. M. Baltrusaitis *et al.* (MARK-III Collaboration), Phys. Rev. Lett. **56**, 2140 (1986).
[25] M. Ablikim *et al.* (BESIII Collaboration), Phys. Rev. D **100**, 072006 (2019).
[26] M. Ablikim *et al.* (BESIII Collaboration), Phys. Rev. D **109**, 072003 (2024).
[27] M. Ablikim *et al.* (BESIII Collaboration), Phys. Lett. B **734**, 227 (2014).
[28] H. Albrecht *et al.* (ARGUS Collaboration), Phys. Lett. B **241**, 278 (1990).
[29] S. S. Wilks, Ann. Math. Stat. **9**, 60 (1938).
[30] M. Ablikim *et al.* (BESIII Collaboration), Phys. Rev. D **92**, 112008 (2015).
[31] J.-Y. Zhang *et al.*, Chin. Phys. C **40**, 076001 (2016).
[32] M. Ablikim *et al.* (BESIII Collaboration), Phys. Rev. D **106**, 092005 (2022).
[33] M. Ablikim *et al.* (BESIII Collaboration), Phys. Rev. D **106**, 032002 (2022).
[34] M. Ablikim *et al.* (BESIII Collaboration), Phys. Rev. D **110**, 052012 (2024).
[35] M. Ablikim *et al.* (BESIII Collaboration), Phys. Rev. D **97**, 072004 (2018).
[36] https://cstr.cn/31109.02.BEPC.

M. Ablikim,[1] M. N. Achasov,[4,b] P. Adlarson,[77] X. C. Ai,[82] R. Aliberti,[36] A. Amoroso,[76a,76c] Q. An,[73,59,†] Y. Bai,[58] O. Bakina,[37] Y. Ban,[47,g] H.-R. Bao,[65] V. Batozskaya,[1,45] K. Begzsuren,[33] N. Berger,[36] M. Berlowski,[45] M. Bertani,[29a] D. Bettoni,[30a] F. Bianchi,[76a,76c] E. Bianco,[76a,76c] A. Bortone,[76a,76c] I. Boyko,[37] R. A. Briere,[5] A. Brueggemann,[70] H. Cai,[78] M. H. Cai,[39,j,k] X. Cai,[1,59] A. Calcaterra,[29a] G. F. Cao,[1,65] N. Cao,[1,65] S. A. Cetin,[63a] X. Y. Chai,[47,g] J. F. Chang,[1,59] G. R. Che,[44] Y. Z. Che,[1,59,65] C. H. Chen,[9] Chao Chen,[56] G. Chen,[1] H. S. Chen,[1,65] H. Y. Chen,[21] M. L. Chen,[1,59,65] S. J. Chen,[43] S. L. Chen,[46] S. M. Chen,[62] T. Chen,[1,65] X. R. Chen,[32,65] X. T. Chen,[1,65] X. Y. Chen,[12,f] Y. B. Chen,[1,59] Y. Q. Chen,[35] Y. Q. Chen,[16] Z. Chen,[25] Z. J. Chen,[26,h] Z. K. Chen,[60] S. K. Choi,[10] X. Chu,[12,f] G. Cibinetto,[30a] F. Cossio,[76c] J. Cottee-Meldrum,[64] J. J. Cui,[51] H. L. Dai,[1,59] J. P. Dai,[80] A. Dbeyssi,[19] R. E. de Boer,[3] D. Dedovich,[37] C. Q. Deng,[74] Z. Y. Deng,[1] A. Denig,[36] I. Denysenko,[37] M. Destefanis,[76a,76c] F. De Mori,[76a,76c] B. Ding,[68,1] X. X. Ding,[47,g] Y. Ding,[41] Y. Ding,[35] Y. X. Ding,[31] J. Dong,[1,59] L. Y. Dong,[1,65] M. Y. Dong,[1,59,65] X. Dong,[78] M. C. Du,[1] S. X. Du,[82] S. X. Du,[12,f] Y. Y. Duan,[56] P. Egorov,[37,a] G. F. Fan,[43] J. J. Fan,[20] Y. H. Fan,[46] J. Fang,[1,59] J. Fang,[60] S. S. Fang,[1,65] W. X. Fang,[1] Y. Q. Fang,[1,59] R. Farinelli,[30a] L. Fava,[76b,76c] F. Feldbauer,[3] G. Felici,[29a] C. Q. Feng,[73,59] J. H. Feng,[16] L. Feng,[39,j,k] Q. X. Feng,[39,j,k] Y. T. Feng,[73,59] M. Fritsch,[3] C. D. Fu,[1] J. L. Fu,[65] Y. W. Fu,[1,65] H. Gao,[65] X. B. Gao,[42] Y. Gao,[73,59] Y. N. Gao,[47,g] Y. N. Gao,[20] Y. Y. Gao,[31] S. Garbolino,[76c] I. Garzia,[30a,30b] L. Ge,[58] P. T. Ge,[20] Z. W. Ge,[43] C. Geng,[60] E. M. Gersabeck,[69] A. Gilman,[71] K. Goetzen,[13] J. D. Gong,[35] L. Gong,[41] W. X. Gong,[1,59] W. Gradl,[36] S. Gramigna,[30a,30b] M. Greco,[76a,76c] M. H. Gu,[1,59] Y. T. Gu,[15] C. Y. Guan,[1,65] A. Q. Guo,[32] L. B. Guo,[42] M. J. Guo,[51] R. P. Guo,[50] Y. P. Guo,[12,f] A. Guskov,[37,a] J. Gutierrez,[28] K. L. Han,[65] T. T. Han,[1] F. Hanisch,[3] K. D. Hao,[73,59] X. Q. Hao,[20] F. A. Harris,[67] K. K. He,[56] K. L. He,[1,65] F. H. Heinsius,[3] C. H. Heinz,[36] Y. K. Heng,[1,59,65] C. Herold,[61] P. C. Hong,[35] G. Y. Hou,[1,65] X. T. Hou,[1,65] Y. R. Hou,[65] Z. L. Hou,[1] H. M. Hu,[1,65] J. F. Hu,[57,i] Q. P. Hu,[73,59] S. L. Hu,[12,f] T. Hu,[1,59,65] Y. Hu,[1] Z. M. Hu,[60] G. S. Huang,[73,59] K. X. Huang,[60] L. Q. Huang,[32,65] P. Huang,[43] X. T. Huang,[51] Y. P. Huang,[1] Y. S. Huang,[60] T. Hussain,[75] N. Hüsken,[36] N. in der Wiesche,[70] J. Jackson,[28] Q. Ji,[1] Q. P. Ji,[20] W. Ji,[1,65] X. B. Ji,[1,65] X. L. Ji,[1,59] Y. Y. Ji,[51] Z. K. Jia,[73,59] D. Jiang,[1,65] H. B. Jiang,[78] P. C. Jiang,[47,g] S. J. Jiang,[9] T. J. Jiang,[17] X. S. Jiang,[1,59,65] Y. Jiang,[65] J. B. Jiao,[51] J. K. Jiao,[35] Z. Jiao,[24] S. Jin,[43] Y. Jin,[68] M. Q. Jing,[1,65] X. M. Jing,[65] T. Johansson,[77] S. Kabana,[34] N. Kalantar-Nayestanaki,[66] X. L. Kang,[9] X. S. Kang,[41] M. Kavatsyuk,[66] B. C. Ke,[82] V. Khachatryan,[28] A. Khoukaz,[70] R. Kiuchi,[1] O. B. Kolcu,[63a] B. Kopf,[3] M. Kuessner,[3] X. Kui,[1,65] N. Kumar,[27] A. Kupsc,[45,77] W. Kühn,[38] Q. Lan,[74] W. N. Lan,[20] T. T. Lei,[73,59] M. Lellmann,[36] T. Lenz,[36] C. Li,[48] C. Li,[44] C. H. Li,[40] C. K. Li,[21] D. M. Li,[82] F. Li,[1,59] G. Li,[1] H. B. Li,[1,65] H. J. Li,[20] H. N. Li,[57,i] Hui Li,[44] J. R. Li,[62] J. S. Li,[60] K. Li,[1] K. L. Li,[20] K. L. Li,[39,j,k] L. J. Li,[1,65] Lei Li,[49] M. H. Li,[44] M. R. Li,[1,65] P. L. Li,[65] P. R. Li,[39,j,k] Q. M. Li,[1,65] Q. X. Li,[51] R. Li,[18,32] S. X. Li,[12] T. Li,[51] T. Y. Li,[44] W. D. Li,[1,65] W. G. Li,[1,†] X. Li,[1,65] X. H. Li,[73,59] X. L. Li,[51] X. Y. Li,[1,8] X. Z. Li,[60] Y. Li,[20]

Y. G. Li,[47,g] Y. P. Li,[35] Z. J. Li,[60] Z. Y. Li,[80] H. Liang,[73,59] Y. F. Liang,[55] Y. T. Liang,[32,65] G. R. Liao,[14] L. B. Liao,[60] M. H. Liao,[60] Y. P. Liao,[1,65] J. Libby,[27] A. Limphirat,[61] C. C. Lin,[56] D. X. Lin,[32,65] L. Q. Lin,[40] T. Lin,[1] B. J. Liu,[1] B. X. Liu,[78] C. Liu,[35] C. X. Liu,[1] F. Liu,[1] F. H. Liu,[54] Feng Liu,[6] G. M. Liu,[57,i] H. Liu,[39,j,k] H. B. Liu,[15] H. H. Liu,[1] H. M. Liu,[1,65] Huihui Liu,[22] J. B. Liu,[73,59] J. J. Liu,[21] K. Liu,[39,j,k] K. Liu,[74] K. Y. Liu,[41] Ke Liu,[23] L. C. Liu,[44] Lu Liu,[44] M. H. Liu,[12,f] P. L. Liu,[1] Q. Liu,[65] S. B. Liu,[73,59] T. Liu,[12,f] W. K. Liu,[44] W. M. Liu,[73,59] W. T. Liu,[40] X. Liu,[39,j,k] X. Liu,[40] X. K. Liu,[39,j,k] X. L. Liu,[12,f] X. P. Liu,[12,f] X. Y. Liu,[78] Y. Liu,[39,j,k] Y. Liu,[82] Yuan Liu,[82] Y. B. Liu,[44] Z. A. Liu,[1,59,65] Z. D. Liu,[9] Z. Q. Liu,[51] X. C. Lou,[1,59,65] F. X. Lu,[60] H. J. Lu,[24] J. G. Lu,[1,59] X. L. Lu,[16] Y. Lu,[7] Y. H. Lu,[1,65] Y. P. Lu,[1,59] Z. H. Lu,[1,65] C. L. Luo,[42] J. R. Luo,[60] J. S. Luo,[1,65] M. X. Luo,[81] T. Luo,[12,f] X. L. Luo,[1,59] Z. Y. Lv,[23] X. R. Lyu,[65,o] Y. F. Lyu,[44] Y. H. Lyu,[82] F. C. Ma,[41] H. L. Ma,[1] J. L. Ma,[1,65] L. L. Ma,[51] L. R. Ma,[68] Q. M. Ma,[1] R. Q. Ma,[1,65] R. Y. Ma,[20] T. Ma,[73,59] X. T. Ma,[1,65] X. Y. Ma,[1,59] Y. M. Ma,[32] F. E. Maas,[19] I. MacKay,[71] M. Maggiora,[76a,76c] S. Malde,[71] Q. A. Malik,[75] H. X. Mao,[39,j,k] Y. J. Mao,[47,g] Z. P. Mao,[1] S. Marcello,[76a,76c] A. Marshall,[64] F. M. Melendi,[30a,30b] Y. H. Meng,[65] Z. X. Meng,[68] G. Mezzadri,[30a] H. Miao,[1,65] T. J. Min,[43] R. E. Mitchell,[28] X. H. Mo,[1,59,65] B. Moses,[28] N. Yu. Muchnoi,[4,b] J. Muskalla,[36] Y. Nefedov,[37] F. Nerling,[19,d] L. S. Nie,[21] I. B. Nikolaev,[4,b] Z. Ning,[1,59] S. Nisar,[11,l] Q. L. Niu,[39,j,k] W. D. Niu,[12,f] C. Normand,[64] S. L. Olsen,[10,65] Q. Ouyang,[1,59,65] S. Pacetti,[29b,29c] X. Pan,[56] Y. Pan,[58] A. Pathak,[10] Y. P. Pei,[73,59] M. Pelizaeus,[3] H. P. Peng,[73,59] X. J. Peng,[39,j,k] Y. Y. Peng,[39,j,k] K. Peters,[13,d] K. Petridis,[64] J. L. Ping,[42] R. G. Ping,[1,65] S. Plura,[36] V. Prasad,[35] F. Z. Qi,[1] H. R. Qi,[62] M. Qi,[43] S. Qian,[1,59] W. B. Qian,[65] C. F. Qiao,[65] J. H. Qiao,[20] J. J. Qin,[74] J. L. Qin,[56] L. Q. Qin,[14] L. Y. Qin,[73,59] P. B. Qin,[74] X. P. Qin,[12,f] X. S. Qin,[51] Z. H. Qin,[1,59] J. F. Qiu,[1] Z. H. Qu,[74] J. Rademacker,[64] C. F. Redmer,[36] A. Rivetti,[76c] M. Rolo,[76c] G. Rong,[1,65] S. S. Rong,[1,65] F. Rosini,[29b,29c] Ch. Rosner,[19] M. Q. Ruan,[1,59] N. Salone,[45] A. Sarantsev,[37,c] Y. Schelhaas,[36] K. Schoenning,[77] M. Scodeggio,[30a] K. Y. Shan,[12,f] W. Shan,[25] X. Y. Shan,[73,59] Z. J. Shang,[39,j,k] J. F. Shangguan,[17] L. G. Shao,[1,65] M. Shao,[73,59] C. P. Shen,[12,f] H. F. Shen,[1,8] W. H. Shen,[65] X. Y. Shen,[1,65] B. A. Shi,[65] H. Shi,[73,59] J. L. Shi,[12,f] J. Y. Shi,[1] S. Y. Shi,[74] X. Shi,[1,59] H. L. Song,[73,59] J. J. Song,[20] T. Z. Song,[60] W. M. Song,[35] Y. J. Song,[12,f] Y. X. Song,[47,g,m] S. Sosio,[76a,76c] S. Spataro,[76a,76c] F. Stieler,[36] S. S. Su,[41] Y. J. Su,[65] G. B. Sun,[78] G. X. Sun,[1] H. Sun,[65] H. K. Sun,[1] J. F. Sun,[20] K. Sun,[62] L. Sun,[78] S. S. Sun,[1,65] T. Sun,[52,e] Y. C. Sun,[78] Y. H. Sun,[31] Y. J. Sun,[73,59] Y. Z. Sun,[1] Z. Q. Sun,[1,65] Z. T. Sun,[51] C. J. Tang,[55] G. Y. Tang,[1] J. Tang,[60] J. J. Tang,[73,59] L. F. Tang,[40] Y. A. Tang,[78] L. Y. Tao,[74] M. Tat,[71] J. X. Teng,[73,59] J. Y. Tian,[73,59] W. H. Tian,[60] Y. Tian,[32] Z. F. Tian,[78] I. Uman,[63b] B. Wang,[1] B. Wang,[60] Bo Wang,[73,59] C. Wang,[39,j,k] C. Wang,[20] Cong Wang,[23] D. Y. Wang,[47,g] H. J. Wang,[39,j,k] J. J. Wang,[78] K. Wang,[1,59] L. L. Wang,[1] L. W. Wang,[35] M. Wang,[51] M. Wang,[73,59] N. Y. Wang,[65] S. Wang,[12,f] T. Wang,[12,f] T. J. Wang,[44] W. Wang,[60] Wei Wang,[74] W. P. Wang,[36,73,59,n] X. Wang,[47,g] X. F. Wang,[39,j,k] X. J. Wang,[40] X. L. Wang,[12,f] X. N. Wang,[1,65] Y. Wang,[62] Y. D. Wang,[46] Y. F. Wang,[1,8,65] Y. H. Wang,[39,j,k] Y. J. Wang,[73,59] Y. L. Wang,[20] Y. N. Wang,[78] Y. Q. Wang,[1] Yaqian Wang,[18] Yi Wang,[62] Yuan Wang,[18,32] Z. Wang,[1,59] Z. L. Wang,[74] Z. L. Wang,[2] Z. Q. Wang,[12,f] Z. Y. Wang,[1,65] D. H. Wei,[14] H. R. Wei,[44] F. Weidner,[70] S. P. Wen,[1] Y. R. Wen,[40] U. Wiedner,[3] G. Wilkinson,[71] M. Wolke,[77] C. Wu,[40] J. F. Wu,[1,8] L. H. Wu,[1] L. J. Wu,[1,65] L. J. Wu,[20] Lianjie Wu,[20] S. G. Wu,[1,65] S. M. Wu,[65] X. Wu,[12,f] X. H. Wu,[35] Y. J. Wu,[32] Z. Wu,[1,59] L. Xia,[73,59] X. M. Xian,[40] B. H. Xiang,[1,65] D. Xiao,[39,j,k] G. Y. Xiao,[43] H. Xiao,[74] Y. L. Xiao,[12,f] Z. J. Xiao,[42] C. Xie,[43] K. J. Xie,[1,65] X. H. Xie,[47,g] Y. Xie,[51] Y. G. Xie,[1,59] Y. H. Xie,[6] Z. P. Xie,[73,59] T. Y. Xing,[1,65] C. F. Xu,[1,65] C. J. Xu,[60] G. F. Xu,[1] H. Y. Xu,[68,2] H. Y. Xu,[2] M. Xu,[73,59] Q. J. Xu,[17] Q. N. Xu,[31] T. D. Xu,[74] W. Xu,[1] W. L. Xu,[68] X. P. Xu,[56] Y. Xu,[41] Y. Xu,[12,f] Y. C. Xu,[79] Z. S. Xu,[65] F. Yan,[12,f] H. Y. Yan,[40] L. Yan,[12,f] W. B. Yan,[73,59] W. C. Yan,[82] W. H. Yan,[6] W. P. Yan,[20] X. Q. Yan,[1,65] H. J. Yang,[52,e] H. L. Yang,[35] H. X. Yang,[1] J. H. Yang,[43] R. J. Yang,[20] T. Yang,[1] Y. Yang,[12,f] Y. F. Yang,[44] Y. H. Yang,[43] Y. Q. Yang,[9] Y. X. Yang,[1,65] Y. Z. Yang,[20] M. Ye,[1,59] M. H. Ye,[8,†] Z. J. Ye,[57,i] Junhao Yin,[44] Z. Y. You,[60] B. X. Yu,[1,59,65] C. X. Yu,[44] G. Yu,[13] J. S. Yu,[26,h] L. Q. Yu,[12,f] M. C. Yu,[41] T. Yu,[74] X. D. Yu,[47,g] Y. C. Yu,[82] C. Z. Yuan,[1,65] H. Yuan,[1,65] J. Yuan,[35] J. Yuan,[46] L. Yuan,[2] S. C. Yuan,[1,65] X. Q. Yuan,[1] Y. Yuan,[1,65] Z. Y. Yuan,[60] C. X. Yue,[40] Ying Yue,[20] A. A. Zafar,[75] S. H. Zeng,[64] X. Zeng,[12,f] Y. Zeng,[26,h] Yujie Zeng,[60] Y. J. Zeng,[1,65] X. Y. Zhai,[35] Y. H. Zhan,[60] Shunan Zhang,[71] A. Q. Zhang,[1,65] B. L. Zhang,[1,65] B. X. Zhang,[1] D. H. Zhang,[44] G. Y. Zhang,[20] G. Y. Zhang,[1,65] H. Zhang,[73,59] H. Zhang,[82] H. C. Zhang,[1,59,65] H. H. Zhang,[60] H. Q. Zhang,[1,59,65]

H. R. Zhang,[73,59] H. Y. Zhang,[1,59] Jin Zhang,[82] J. Zhang,[60] J. J. Zhang,[53] J. L. Zhang,[21] J. Q. Zhang,[42] J. S. Zhang,[12,f] J. W. Zhang,[1,59,65] J. X. Zhang,[39,j,k] J. Y. Zhang,[1] J. Z. Zhang,[1,65] Jianyu Zhang,[65] L. M. Zhang,[62] Lei Zhang,[43] N. Zhang,[82] P. Zhang,[1,8] Q. Zhang,[20] Q. Y. Zhang,[35] R. Y. Zhang,[39,j,k] S. H. Zhang,[1,65] Shulei Zhang,[26,h] X. M. Zhang,[1] X. Y. Zhang,[41] X. Y. Zhang,[51] Y. Zhang,[1] Y. Zhang,[74] Y. T. Zhang,[82] Y. H. Zhang,[1,59] Y. M. Zhang,[40] Y. P. Zhang,[73,59] Z. D. Zhang,[1] Z. H. Zhang,[1] Z. L. Zhang,[35] Z. L. Zhang,[56] Z. X. Zhang,[20] Z. Y. Zhang,[78] Z. Y. Zhang,[44] Z. Z. Zhang,[46] Zh. Zh. Zhang,[20] G. Zhao,[1] J. Y. Zhao,[1,65] J. Z. Zhao,[1,59] L. Zhao,[1] L. Zhao,[73,59] M. G. Zhao,[44] N. Zhao,[80] R. P. Zhao,[65] S. J. Zhao,[82] Y. B. Zhao,[1,59] Y. L. Zhao,[56] Y. X. Zhao,[32,65] Z. G. Zhao,[73,59] A. Zhemchugov,[37,a] B. Zheng,[74] B. M. Zheng,[35] J. P. Zheng,[1,59] W. J. Zheng,[1,65] X. R. Zheng,[20] Y. H. Zheng,[65,o] B. Zhong,[42] C. Zhong,[20] H. Zhou,[36,51,n] J. Q. Zhou,[35] J. Y. Zhou,[35] S. Zhou,[6] X. Zhou,[78] X. K. Zhou,[6] X. R. Zhou,[73,59] X. Y. Zhou,[40] Y. X. Zhou,[79] Y. Z. Zhou,[12,f] A. N. Zhu,[65] J. Zhu,[44] K. Zhu,[1] K. J. Zhu,[1,59,65] K. S. Zhu,[12,f] L. Zhu,[35] L. X. Zhu,[65] S. H. Zhu,[72] T. J. Zhu,[12,f] W. D. Zhu,[42] W. D. Zhu,[12,f] W. J. Zhu,[1] W. Z. Zhu,[20] Y. C. Zhu,[73,59] Z. A. Zhu,[1,65] X. Y. Zhuang,[44] J. H. Zou,[1] and J. Zu[73,59]

(BESIII Collaboration)

[1]*Institute of High Energy Physics, Beijing 100049, People's Republic of China*
[2]*Beihang University, Beijing 100191, People's Republic of China*
[3]*Bochum Ruhr-University, D-44780 Bochum, Germany*
[4]*Budker Institute of Nuclear Physics SB RAS (BINP), Novosibirsk 630090, Russia*
[5]*Carnegie Mellon University, Pittsburgh, Pennsylvania 15213, USA*
[6]*Central China Normal University, Wuhan 430079, People's Republic of China*
[7]*Central South University, Changsha 410083, People's Republic of China*
[8]*China Center of Advanced Science and Technology, Beijing 100190, People's Republic of China*
[9]*China University of Geosciences, Wuhan 430074, People's Republic of China*
[10]*Chung-Ang University, Seoul, 06974, Republic of Korea*
[11]*COMSATS University Islamabad, Lahore Campus, Defence Road, Off Raiwind Road, 54000 Lahore, Pakistan*
[12]*Fudan University, Shanghai 200433, People's Republic of China*
[13]*GSI Helmholtzcentre for Heavy Ion Research GmbH, D-64291 Darmstadt, Germany*
[14]*Guangxi Normal University, Guilin 541004, People's Republic of China*
[15]*Guangxi University, Nanning 530004, People's Republic of China*
[16]*Guangxi University of Science and Technology, Liuzhou 545006, People's Republic of China*
[17]*Hangzhou Normal University, Hangzhou 310036, People's Republic of China*
[18]*Hebei University, Baoding 071002, People's Republic of China*
[19]*Helmholtz Institute Mainz, Staudinger Weg 18, D-55099 Mainz, Germany*
[20]*Henan Normal University, Xinxiang 453007, People's Republic of China*
[21]*Henan University, Kaifeng 475004, People's Republic of China*
[22]*Henan University of Science and Technology, Luoyang 471003, People's Republic of China*
[23]*Henan University of Technology, Zhengzhou 450001, People's Republic of China*
[24]*Huangshan College, Huangshan 245000, People's Republic of China*
[25]*Hunan Normal University, Changsha 410081, People's Republic of China*
[26]*Hunan University, Changsha 410082, People's Republic of China*
[27]*Indian Institute of Technology Madras, Chennai 600036, India*
[28]*Indiana University, Bloomington, Indiana 47405, USA*
[29a]*INFN Laboratori Nazionali di Frascati, INFN Laboratori Nazionali di Frascati, I-00044, Frascati, Italy;*
[29b]*INFN Laboratori Nazionali di Frascati, INFN Sezione di Perugia, I-06100, Perugia, Italy;*
[29c]*INFN Laboratori Nazionali di Frascati, University of Perugia, I-06100, Perugia, Italy*
[30a]*INFN Sezione di Ferrara, INFN Sezione di Ferrara, I-44122, Ferrara, Italy;*
[30b]*INFN Sezione di Ferrara, University of Ferrara, I-44122, Ferrara, Italy*
[31]*Inner Mongolia University, Hohhot 010021, People's Republic of China*
[32]*Institute of Modern Physics, Lanzhou 730000, People's Republic of China*
[33]*Institute of Physics and Technology, Mongolian Academy of Sciences, Peace Avenue 54B, Ulaanbaatar 13330, Mongolia*
[34]*Instituto de Alta Investigación, Universidad de Tarapacá, Casilla 7D, Arica 1000000, Chile*
[35]*Jilin University, Changchun 130012, People's Republic of China*

[36]Johannes Gutenberg University of Mainz, Johann-Joachim-Becher-Weg 45, D-55099 Mainz, Germany
[37]Joint Institute for Nuclear Research, 141980 Dubna, Moscow region, Russia
[38]Justus-Liebig-Universitaet Giessen, II. Physikalisches Institut, Heinrich-Buff-Ring 16, D-35392 Giessen, Germany
[39]Lanzhou University, Lanzhou 730000, People's Republic of China
[40]Liaoning Normal University, Dalian 116029, People's Republic of China
[41]Liaoning University, Shenyang 110036, People's Republic of China
[42]Nanjing Normal University, Nanjing 210023, People's Republic of China
[43]Nanjing University, Nanjing 210093, People's Republic of China
[44]Nankai University, Tianjin 300071, People's Republic of China
[45]National Centre for Nuclear Research, Warsaw 02-093, Poland
[46]North China Electric Power University, Beijing 102206, People's Republic of China
[47]Peking University, Beijing 100871, People's Republic of China
[48]Qufu Normal University, Qufu 273165, People's Republic of China
[49]Renmin University of China, Beijing 100872, People's Republic of China
[50]Shandong Normal University, Jinan 250014, People's Republic of China
[51]Shandong University, Jinan 250100, People's Republic of China
[52]Shanghai Jiao Tong University, Shanghai 200240, People's Republic of China
[53]Shanxi Normal University, Linfen 041004, People's Republic of China
[54]Shanxi University, Taiyuan 030006, People's Republic of China
[55]Sichuan University, Chengdu 610064, People's Republic of China
[56]Soochow University, Suzhou 215006, People's Republic of China
[57]South China Normal University, Guangzhou 510006, People's Republic of China
[58]Southeast University, Nanjing 211100, People's Republic of China
[59]State Key Laboratory of Particle Detection and Electronics, Beijing 100049, Hefei 230026, People's Republic of China
[60]Sun Yat-Sen University, Guangzhou 510275, People's Republic of China
[61]Suranaree University of Technology, University Avenue 111, Nakhon Ratchasima 30000, Thailand
[62]Tsinghua University, Beijing 100084, People's Republic of China
[63a]Turkish Accelerator Center Particle Factory Group, Istinye University, 34010, Istanbul, Turkey;
[63b]Turkish Accelerator Center Particle Factory Group, Near East University, Nicosia, North Cyprus, 99138, Mersin 10, Turkey
[64]University of Bristol, H H Wills Physics Laboratory, Tyndall Avenue, Bristol, BS8 1TL, United Kingdom
[65]University of Chinese Academy of Sciences, Beijing 100049, People's Republic of China
[66]University of Groningen, NL-9747 AA Groningen, The Netherlands
[67]University of Hawaii, Honolulu, Hawaii 96822, USA
[68]University of Jinan, Jinan 250022, People's Republic of China
[69]University of Manchester, Oxford Road, Manchester, M13 9PL, United Kingdom
[70]University of Muenster, Wilhelm-Klemm-Strasse 9, 48149 Muenster, Germany
[71]University of Oxford, Keble Road, Oxford OX13RH, United Kingdom
[72]University of Science and Technology Liaoning, Anshan 114051, People's Republic of China
[73]University of Science and Technology of China, Hefei 230026, People's Republic of China
[74]University of South China, Hengyang 421001, People's Republic of China
[75]University of the Punjab, Lahore-54590, Pakistan
[76a]University of Turin and INFN, University of Turin, I-10125, Turin, Italy;
[76b]University of Turin and INFN, University of Eastern Piedmont, I-15121, Alessandria, Italy;
[76c]University of Turin and INFN, INFN, I-10125, Turin, Italy
[77]Uppsala University, Box 516, SE-75120 Uppsala, Sweden
[78]Wuhan University, Wuhan 430072, People's Republic of China
[79]Yantai University, Yantai 264005, People's Republic of China
[80]Yunnan University, Kunming 650500, People's Republic of China
[81]Zhejiang University, Hangzhou 310027, People's Republic of China
[82]Zhengzhou University, Zhengzhou 450001, People's Republic of China

[†]Deceased.
[a]Also at the Moscow Institute of Physics and Technology, Moscow 141700, Russia.
[b]Also at the Novosibirsk State University, Novosibirsk, 630090, Russia.
[c]Also at the NRC "Kurchatov Institute," PNPI, 188300, Gatchina, Russia.
[d]Also at Goethe University Frankfurt, 60323 Frankfurt am Main, Germany.

[e]Also at Key Laboratory for Particle Physics, Astrophysics and Cosmology, Ministry of Education; Shanghai Key Laboratory for Particle Physics and Cosmology; Institute of Nuclear and Particle Physics, Shanghai 200240, People's Republic of China.
[f]Also at Key Laboratory of Nuclear Physics and Ion-beam Application (MOE) and Institute of Modern Physics, Fudan University, Shanghai 200443, People's Republic of China.
[g]Also at State Key Laboratory of Nuclear Physics and Technology, Peking University, Beijing 100871, People's Republic of China.
[h]Also at School of Physics and Electronics, Hunan University, Changsha 410082, China.
[i]Also at Guangdong Provincial Key Laboratory of Nuclear Science, Institute of Quantum Matter, South China Normal University, Guangzhou 510006, China.
[j]Also at MOE Frontiers Science Center for Rare Isotopes, Lanzhou University, Lanzhou 730000, People's Republic of China.
[k]Also at Lanzhou Center for Theoretical Physics, Lanzhou University, Lanzhou 730000, People's Republic of China.
[l]Also at the Department of Mathematical Sciences, IBA, Karachi 75270, Pakistan.
[m]Also at Ecole Polytechnique Federale de Lausanne (EPFL), CH-1015 Lausanne, Switzerland.
[n]Also at Helmholtz Institute Mainz, Staudinger Weg 18, D-55099 Mainz, Germany.
[o]Also at Hangzhou Institute for Advanced Study, University of Chinese Academy of Sciences, Hangzhou 310024, China.